# Channel Adjustment of a Gravel-bed Stream under Episodic Sediment Supply Regimes

by

Maria Alejandra Elgueta

A THESIS SUBMITTED IN PARTIAL FULFILLMENT OF
THE REQUIREMENTS FOR THE DEGREE OF

**Master of Science**

in

THE FACULTY OF GRADUATE AND POSTDOCTORAL STUDIES

(Geography)

The University of British Columbia

(Vancouver)

January 2014

# Abstract

Sediment supply is a key control on sediment transport rates and bed evolution in a stream. This study examined the adjustment of a gravel-bed stream under episodic sediment supply regimes by conducting a flume experiment in the Mountain Channel Hydraulic Experimental Laboratory at the University of British Columbia. The experiment consisted of a sequence of runs with no feed, constant feed and episodic supply regimes; but constant water discharge and feed texture. The observations indicated that sediment transport rates, the texture of bedload and the bed surface, sediment storage, bed slope, and bed topography adjusted to changes in sediment supply. The relative mobility of sediment instead did not change significantly. Under constant feed, transport rates showed a slow and small increase. The texture of the surface was fluctuating, the same as of the bedload. Sediment storage was relatively large, and the bed slope presented small changes. If the same amount of sediment entered in one or few pulses, transport rates and the texture of the surface exhibited pronounced changes just after the pulse, and returned to conditions similar to previous the pulse after some time. The size of the pulses influenced the results, and larger pulses caused larger increases of transport rates and finer textures on the bed surface. Cumulative storage, bed slope and bed morphology adjusted to episodic supply; but did not return to the conditions before the pulse, revealing that the effects of sediment supply over the bed were cumulative and persisted under periods of no feed. During these periods, transport rates decreased, the bed texture coarsened, and there was little change in the bed slope. After few hours of no feed, transport rates were relatively low and changes in elevation were small. Our results suggested that episodic supply produced interesting patterns of channel adjustment (different from constant feed regimes) that depend on the size and frequency of the supply.

# Preface

This thesis is based on a flume experiment conducted in the Mountain Channel Hydraulic Experimental Laboratory (UBC), in collaboration with C. von Flotow and T. Müller, and under the supervision of M. Hassan. We set and tested most of the equipment in the flume and collected all of the data.

Labview codes for data collection with the light table and bed scans were written by A. Zimmermann and modified by us. S. Chartrand assisted us to improve the design of the outlet of the flume. Undergraduate students helped us to paint and sieve sediment.

I conducted all the data analysis presented in this thesis and wrote the manuscript. Claudia von Flotow used the same data for her MSc thesis, but conducted her own analysis ( see von Flotow, 2013 in the References).

# Table of contents

# List of tables

# List of figures

## Acknowledgements

I thank my supervisor Marwan Hassan who gave me the chance to play with the flume, and express my gratitude to Claudia von Flotow and Tobias Müller who worked with me and next to me in this big task. I thank Carles Ferrer and Shawn Chartrand for their good advice and useful comments; and Andre Zimmermann for helping me each time the Labview codes did not work. I appreciate the technical support from Rick Ketler and Ivan Liu; and Helena's help in sieving that was always the worse task. I would also like to thank Katie DeRego for helping me with the manuscript edition and improving my scientific English.

I thank my family. Especially my son and husband that reminded me that life is beautiful even when things don't go as planned. I thank my parents and my aunt for encouraging me to study; and my neighbours and friends who helped me during these two years.

# Chapter 1: Introduction

The transport patterns of stream bed sediment largely determine channel morphology and are important for stream ecology and the maintenance of human infrastructures in fluvial environments. Channel morphology is key in the suitability of benthic habitat for stream organisms (Lisle, 1989), such as salmon and trout that build redds in specific locations of the channel. Good knowledge of the processes of sediment transport is important for the planning and safety of built environments in streams. For example, flow in culverts and around bridge piers can cause erosion of the bed, damaging the environment and exposing the foundations of the structure. Or, the discharge of sediment in a reservoir formed by a dam might cause filling, requiring the removal of the dam. Sediment transport is also useful for quantifying changes in the channel, i.e. bank erosion (Green et al., 1999), and at a larger scale for understanding landscape evolution (Roering et al., 1999; Whipple & Tucker, 2002).

The transport of sediment in a stream bed is controlled by hydraulic conditions and the sediment supply regime. The water flow distribution over the bed defines the pattern of sediment transport rates, which changes the bed by erosion or deposition of sediment. In turn, changes in the bed induce variations in the flow field and transport patterns. Estimations of transport rates using hydraulically based relations in gravel-bed rivers are often inaccurate, primarily because models are based on average hydraulic relations and do not consider the fluctuation in flow, patterns of sediment supply and bed surface structuring. These effects are probably large because variations of more than two orders of magnitude have been observed in transport rates under constant flow (Hayward, 1980; Jackson & Beschta, 1982). Sediment inputs cause important changes in the bed morphology and bed surface composition (texture and structure), affecting the availability of sediment for transport, as well as the distribution of shear stress over the bed.

The transport-storage relations in a stream are controlled by sediment supply. The same flow events can produce different transport rates due to changes in sediment storage and bed surface composition (e.g. Buffington & Montgomery, 1999). When sediment supply is low, a coarse, well-structured bed develops and sediment transport rates are low (Parker et al., 1982; Dietrich et al., 1989; Church et al., 1998; Ryan, 2001; Church & Hassan, 2002; Hassan & Woodsmith, 2004). Streams with relatively large sediment supply have finer bed surfaces with poorly developed structures and higher transport rates ( Lisle & Madej, 1992).

The adjustment of a channel to changes in sediment supply is conditioned by the way in which the sediment enters the system (i.e. supply rates and duration, size and frequency of the events). Most experimental work has been conducted under a constant feed regime where sediment supply is assumed steady over time. These conditions are not representative of mountain gravel bed streams, which are likely to receive supply episodically from the adjacent slopes. These episodes usually consist of large pulses caused by mass movement or large bank collapse. Depending on the texture of the material and flow competence, the sediment can be transferred immediately downstream and have little impact on channel morphology, or it may be stored within the channel (Goff & Ashmore,1994; Lane et al., 1995; Reid & Dunne, 2003)for long periods of time. These streams can shift from supply limited to transport limited depending on the amount and the timing of the episodic supply (Hassan & Zimmermann, 2011). The grain size distribution (GSD) of the sediment feed relatively to the GSD of the bed is important for sediment mobility and the development of bed surface armouring. If a high proportion of relatively fine material is supplied to a reach, sediment transport is likely to increase (Wilcock & Crowe, 2003; Venditti et al., 2010). If the supply instead is composed mainly of coarse material, there could be coarsening of the bed surface and further stabilization.

The main objective of this study is to examine the impact of episodic sediment supply on sediment mobility, bed evolution and channel morphology.

Specifically, we are concerned about:

1. How sediment supply regime is likely to influence transport rates, relative mobility, the texture of the bed surface, sediment storage, bed slope and bed morphology.
2. The implications of the magnitude and frequency of sediment episodes in the adjustment of the variables mentioned above.
3. The importance of the initial bed for the adjustment of the channel to changes in sediment supply.

To achieve the research goals we conducted a flume experiment that combined different feed regimes, but had constant water discharge and feed GSD. The flume allowed us to take high resolution measurements of sediment transport rate, bed elevation and bed surface texture, and to explore patterns under the different supply conditions.

# Chapter 2: Literature review

## 1.1 Sediment transport

Sediment can be transported in suspension, traction or saltation, depending on flow strength and particle size. Very fine material, as silt and clay, are usually considered as wash material, that once entrained is transported for long distances in suspension. Washload is found only in minor quantities in the bed of the river, but may form a significant fraction of upper bank and floodplain deposits. Coarse material as gravel, cobble or boulder, is mobilized by traction mechanisms and is considered as bed material. Bed material load forms the bed and lower banks of a river, and strongly influences the channel morphology.

The threshold for initial motion is needed for transport estimations and is usually represented in the equations by a critical value of mean boundary shear stress. There are important challenges in estimating this critical value of shear stress: (1)shear stress cannot be estimated directly and it has to be back calculated from flow velocity, (2) the spatial variability of flow velocities over an area of the bed is important and defining where to take measurements to get a representative average is not simple task, (3) the threshold varies with particle size, (4) defining the threshold requires an assumption of what will be considered as no motion or zero transport (because of the probabilistic nature of sediment transport). In gravel bed rivers, this threshold has been estimated as a reference shear stress that produces a very small reference transport rate (Parker et al., 1982; Wilcock, 1992; Wilcock & McArdell, 1993) or inferred from the maximum particle size transported under a given shear stress (Andrews, 1983; Ashworth & Ferguson, 1989). By this definition, sediment transport starts when the boundary shear stress exceeds the reference shear stress.

Shields (1936) defined a dimensionless shear stress, known as Shields number ($\tau^*$) that relates the boundary shear stress to the gravity forces acting on a grain of a given size. This is shown in Equation 0.1, where $\tau_b$ is the boundary shear stress, $\rho_s$ is sediment density, $\rho$ is water density, $g$ is gravitational acceleration, and $D$ is particle size.

$$\tau^* = \frac{\tau_b}{(\rho_s - \rho)gD} \qquad 0.1$$

Using uniform sediment, Shields observed that for particles larger than 5 mm (under fully turbulent flow), the shear stress required to entrain a grain was proportional to the size of the

grain. For this reason, the critical Shields number for grains of different sizes was constant at a value of 0.056. Shields approach is used, but the original critical Shields number did not produce accurate predictions in poorly sorted beds, as it didn't consider the effects of sediment mixtures. In sediment mixtures, the interactions of grains of different sizes produce significant effects on entrainment. The relative exposure of grains affects the probability of entrainment as suggested by Einstein (1950), who developed an empirical relation to describe the hiding effect that relatively large particles produce on smaller particles. The hiding factor was a function of the particle diameter to a characteristic diameter of the mixture, for example, the median particle size ($D_{50}$). The critical shear stress for entrainment can also decrease if particle exposure increases (Fenton & Abott, 1977). If hiding and protrusion effects are strong, particles within a wide range of sizes could be entrained at nearly the same critical shear stress. This form of transport has been referred to as equal mobility (Parker & Klingeman, 1982; Andrews, 1983). When estimating the critical shear stress for sediment mixtures a characteristic particle size needs to be specified (i.e. geometric mean or $D_{50}$) and a hiding function applied. A value of 0.045 has been suggested for the entrainment of the $D_{50}$ in gravel beds.

A higher proportion of sand on the bed surface can reduce the critical shear stress for the entrainment of gravels (Wilcock & Crowe, 2003; Curran & Wilcock, 2005). More recent studies have shown the critical Shields stress for entrainment is also affected by channel slope. Grains of the same size require a higher stress for entrainment at steeper slopes; grain emergence and changes in local flow velocity and turbulent fluctuations are responsible for this slope dependency (Lamb et al., 2008).

Spatial and temporal variability of bedload transport rates have been linked to sediment supply in rivers (Trimble, 1981; Meade, 1982; Beschta, 1983). To address the issue of transport rate variability, different stages related to the intensity of sediment transport have been recognized. Two stage (Jackson & Beschta, 1982; Andrews, 1983) and three stage transport models have been presented (Ashworth & Ferguson, 1989; Wilcock & McArdell, 1993). In stage I (Figure 0.1), fine material is mobile over a static bed. This material could be stored in the system or supplied from adjacent slopes. Stage 2 represents partial mobility. Sediment is locally mobilized and the intensity of transport is relatively low. Size selective transport is important and mobility is highly influenced by bed surface structuring. The third stage represents high sediment transport intensity during

relatively large events. Most of the bed surface moves and nearly equal mobility (Parker & Klingeman, 1982; Andrews, 1983) is approximated.

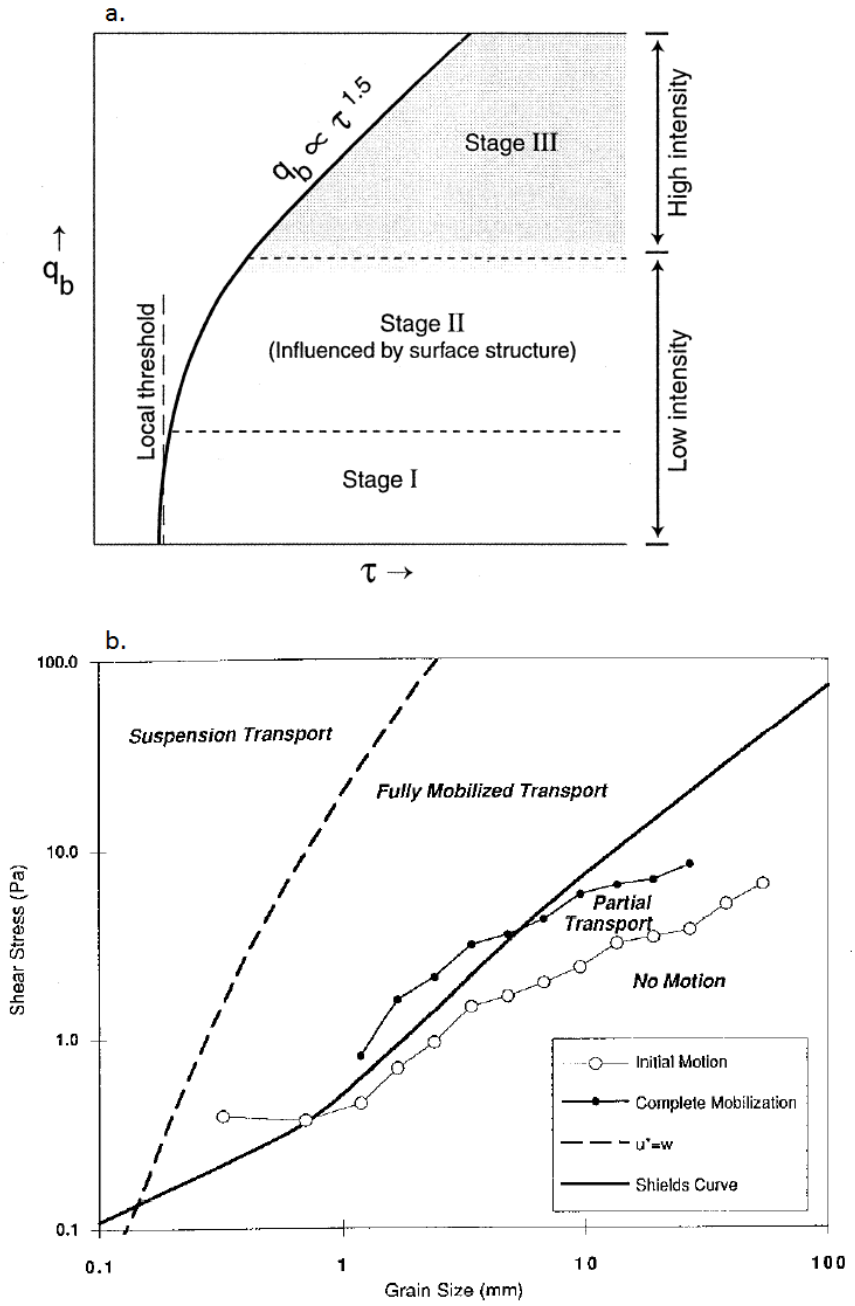


**Figure 0.1. Stages of sediment transport. (a) Schematic diagram of sediment transport rate versus shear stress for varying grain sizes (Hassan et al. 2005). (b) Domains of bedload transport defined in terms of shear stress versus grain size (Wilcock & McArdell, 1993).**

The different grain sizes on the bed surface can move in different proportions. To analyze the relative mobility of grains in a sediment mixture, the limit between grains under partial transport

and those under full mobility can be identified using surface based fractional transport rates (Wilcock & McArdell, 1993). A given grain size ($D_i$) is under partial transport if the ratio between its proportion in transport ($P_i$) and its proportion on the bed surface ($F_i$) is less than one. A grain size is considered fully mobile if the transport ratio is equal to or larger than one. Wilcock & McArdell observed that for a given size, the critical stress required for full mobility was about twice the shear stress required for entrainment of the same size. The limit between partial and full mobility can be significantly affected by changes in the flow (at higher discharges more sizes become fully mobile), but the effects that changes in sediment supply (amounts and texture) produce on relative mobility have not been studied.

## 1.2 Channel adjustment to changes in sediment supply

The temporal and spatial variation in the amount of within-channel sediment storage depends on the supply from external sources (Swanson et al., 1982; Benda, 1990). Changes in the sediment supply regime are followed by adjustments of the channel and sediment transport-storage relations in the system. There are studies that suggest bed states (Church, 1978) and transport regimes of a stream are controlled by the sediment supply regime (as summarized in Hassan et al., 2008). When sediment supply is low, a coarse well-structured bed develops and sediment transport rates are low (Parker & Klingeman, 1982; Dietrich et al., 1989; Church et al., 1998; Hassan & Church, 2000; Ryan, 2001; Church & Hassan, 2002; Hassan & Woodsmith, 2004). Streams with relatively large sediment supply have finer bed surfaces with poorly developed structures and higher transport rates for a given discharge than channels with the same slope, but lower sediment supply ( Lisle & Madej, 1992). Sediment inputs modify the channel morphology and bed surface composition (texture and structure), which affects local sediment transport rates and the distribution of shear stress acting on the bed.

Experimental observations in a stream table (model used to simulate river and watershed systems) suggested that depending on the nature of stream boundaries, channels adjust differently to changes in sediment supply (Eaton, 2004; Eaton & Church, 2009). Non-constrained channels exhibited a primary adjustment of channel sinuosity and reach slope to changes in sediment supply. These systems tended to find the minimum slope capable to transport the sediment supply, which increased flow resistance in the system. An equilibrium range of slopes for a given system could be predicted by a linear function of sediment concentration ($Q_b/Q$), which is limited by the minimum stream power capable of deforming the bed and the maximum sediment feed

that can be transported by the system. In constrained channels with non-erodible banks where lateral migration is not allowed, the response was first by changes in the bed state.

The texture of the bed surface is sensitive to changes in sediment supply. Gravel beds under low supply regimes often exhibit a relatively coarse grained bed surface layer (or armor) over a finer bed subsurface. The degree of armoring is usually represented as the ratio between the median particle size of the bed surface ($D_{50surf}$) and the median grain size of the subsurface ($D_{50sub}$) or bulk material. Armored layers were described downstream of dams (Gessler, 1971; Little & Mayer, 1976) and documented at inactive transport stages in gravel streams, such as Oak Creek, Oregon (Milhous, 1973). Armor can develop under low supply or starvation conditions due to winnowing of fine material. Armour can also develop due to sediment mobility and vertical sorting (Parker & Klingeman, 1982). The latter implies that the fine material goes below the surface while the coarse material remains on the surface, providing an equalizing transport mechanism, by exposing proportionally more the larger grains to the flow, and hiding the smaller ones. Experimental studies suggest that the armor layer remains and varies little under a wide range of flow conditions (Parker & Klingeman, 1982; Parker et al., 1982; Wilcock et al., 2001). Andrews & Erman (1986) found that an armored surface, similar to the one observed at low flow, remained after a snowmelt storm in Sagahen Creek, USA. Wilcock & Detemple (2005) noticed there was no significant change in the bed surface grain size distribution before and after a flood in Oak Creek. The issue was explored through a 1D numerical model in Parker et al., 2008. They observed that over the great majority of the modelled reach, bed elevations and surface grain size distributions were almost invariant at different flows (only a small area upstream exhibited significant change on these variables), and the response to changes in the flow occurred in bedload transport rates and GSDs.

Dietrich et al. (1989) proposed that the bed surface gets coarser when local bedload supply from upstream is less than the capacity of the flow to transport that load. In flume experiments, they observed that at higher transport rates, bedload sheets were present and an alternation of congested (coarse), smooth (fine) and transitional zones migrating downstream. As supply was reduced, the sheets became less frequent, coarser zones expanded, and transport was confined to a progressively narrower fine-textured active zone. Similar results were obtained by Madej et al. (2009) from a model of Redwood Creek that revealed that the bed surface texture got finer with increasing feed rate and coarser if feed rate was decreased, and by Nelson et al. (2009) who

observed that a reduction in supply promoted the development of coarse fixed patches and the reduction of finer mobile patches.

As degradation proceeds in a system, larger particles on the bed can be organized into structures that limit sediment transport, such as stone cells (Hassan & Church, 2000). In natural channels, bed structuring is considered as an evidence of low sediment supply regimes and stable bed elevation (Church et al., 1998). The larger grains that remain on the surface because of the armoring process are usually mobilized for very short distances and rearrange, forming stone clusters (Brayshaw, 1984; Church et al., 1998; Oldmeadow & Church, 2006). Clusters can be broadly defined as discrete, organized groupings of particles that sit above the average elevation of the surrounding bed surface, and can be characterized in terms of their shape, geometric properties and spatial arrangement on the horizontal plane (Strom & Papanicolaou, 2008). Papanicolaou et al. (2012) applied the box-counting method for analyzing cluster morphology from laboratory and field datasets. They suggested that fractals can be powerful and easy to use descriptors of riverbed microforms. Strom & Papanicolaou (2007) observed through field studies that clusters change the nature of turbulent energy production from that of standard boundary layer theory by shifting the region of maximum production of turbulent kinetic energy from the bed to the detached shear layer that is generated at the top of the cluster.

Transport-storage relations over a river reach are affected by changes in sediment supply. Any change in the rate of sediment supply results in a change in stored volume as well as transport rate, which is regulated by channel adjustments. Lisle & Church (2002) proposed a two phase model to explain transport-storage relations in degrading gravel bed channels that was supported with published field studies, flume experiments and simulations. In an initial phase, the primary response of the channel to the reduction in sediment supply is through changes in storage (reductions in sediment stored volume). Bed forms are still present (armoring is absent) and there is no significant decrease in transport rates (sediment output is high and pulsating). During a second phase, transport rates decline significantly and are less variable as the bed armors. The transition to the second phase occurs when the development of bed forms stopped and all of them had exited the flume.

More recently, Smith-Pryor et al. (2011), by modeling cycles in Cuneo Creek, observed that the channel response to degradation was strongly influenced by the channel conditions achieved during the previous aggradation period. If the channel was in equilibrium prior to a feed reduction

and sediment feed was low, degradation immediately transitioned to Lisle and Church's second phase of transport-storage relations; otherwise, the first phase was also present. Channel degradation progressed through three stages: bar building and surface sorting, channel incision, and lateral erosion. They suggested that slight changes in gradient indicate that the adjustment to sediment supply can be mostly attributed to bed texture and channel morphology, as observed by Lisle et al. (1993) and Nelson et al. (2009).

Changes in the grain size distribution (GSD) of sediment supply also produce adjustments in the system. The GSD of feed material relative to the bed influences sediment mobility. A higher proportion of sand in the feed reduces the shear stress required for the entrainment of gravels (Wilcock & Crowe, 2003; Curran & Wilcock, 2005), and finer gravel shows the same effect over coarser fractions (Venditti et al., 2010a, 2010b).

## 1.3 Episodic supply

Most of the experimental studies directed toward understanding the adjustment of fluvial channels to changes in sediment supply have used constant feed regimes, but mountain gravel bed streams usually receive episodic sediment supply. Large sediment pulses can occur through anthropogenic disturbances (Gilbert, 1917; Wolman, 1967) or by natural geomorphic processes such as landslides or debris flows from tributaries (Roberts & Church, 1986; Madej & Ozaki, 1996; Lisle et al., 2001). The introduced material can be deposited (Goff & Ashmore, 1994; Lane et al., 1995; Reid & Dunne, 2003) to be remobilized later (Jackson & Beschta, 1982; Sutherland et al., 2002), or it can be transported and deposited further downstream. The dynamics of episodic pulses of sediment control bed evolution and sediment transport in gravel-bed streams and are key to understanding their long-term dynamics.

The transport capacity of a channel is highly variable at intermediate time scales that correspond with the passage of sediment waves, which change transport capacity-storage relations (Lisle & Church, 2002). Sediment waves are temporary zones of sediment accumulation created by large sediment inputs. In gravel bed channels, their evolution is predominantly dispersive, but some translation is likely to occur if the wave material is considerably finer than the bed material (Lisle et al., 2001; Sklar et al., 2009). Low amplitude bedforms that develop by sediment sorting patterns in poorly sorted sediment systems have been referred to as sediment sheets. They migrate downstream and have been described by a catch and mobilize process in which large grains are

caught in the wakes of other large grains. This is followed by infilling of their interstices by smaller particles, which can in turn smooth out hydraulic wakes causing large particles to be remobilized (Whiting et al., 1988; Venditti et al., 2008). Experimental evidence suggests that the occurrence of bedload sheets, their dimensions, and their dynamics are primarily controlled by sediment supply (Venditti et al., 2008). The addition of sediment pulses to a river became a common practice in rivers where dams and gravel mining eliminated sediment supply and lead to coarse immobile beds of poor habitat quality (Bunte, 2004; Harvey et al., 2005). The importance of the GSD and size of a pulse in mobilizing coarser sediment from the bed has been explored in flume experiments (Sklar et al., 2009; Venditti et al., 2010a, 2010b).

# Chapter 3: Methods

## 2.1 Experimental design

The experiment was conducted in a flume in the Mountain Channel Hydraulic Experimental Laboratory at the University of British Columbia (UBC). The flume is a generic 1:3 model of riffle-pool reaches in East Creek, a mountain stream in UBC's Malcolm Knapp Research Forest. The dimensions of the flume are: 18 m working length, 1 m wide and 1 m deep. The flume slope was set constant at 0.0218 m/m. The grain size distribution (GSD) of the bed material was obtained from two segments in East Creek. The sediment was poorly sorted and encompassed grains from 0.5 mm to 64 mm (Figure 2.1). Grains were classified in ½ phi intervals and painted different colors to facilitate grain size identification on bed surface photos. Twelve meters of the flume were covered with a 10 cm thick layer of sediment to create a well-mixed and leveled initial bed. Fixed gravels epoxied to plywood were placed along four meters upstream of the bed, to condition the flow before it acted on the bed.

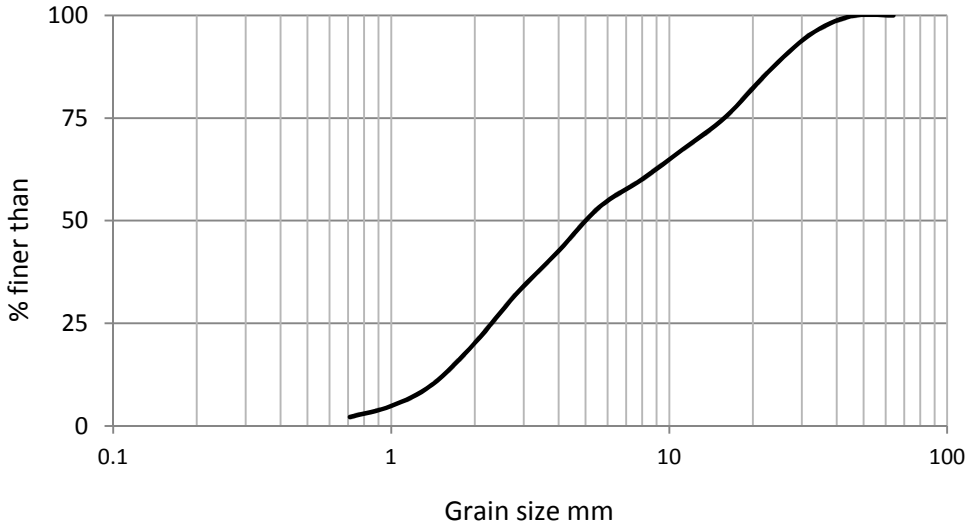


**Figure 2.1. Cumulative grains size distribution of the bed material. The same GSD was used for the feed.**

As the interest was to study channel adjustment to changes in sediment supply, water discharge was set constant at 65 L/s, which was similar to bankfull discharge in the prototype stream. A sequence of seven runs with no feed, constant feed and episodic feed regimes was conducted. Each run lasted 40 hours and followed sequentially as presented in Figure 2.2. The initial bed at Run 1 was a manually prepared, well-mixed and flat bed. For the rest of the runs, the initial bed

was the final bed of the previous run. The sequence of runs made comparisons more difficult than if each run started from the same bed surface conditions, but it also gave time for the bed to evolve and become more realistic. The texture of the feed was constant and had the same GSD of the initial bed to reproduce the material from natural episodic inputs such as debris flow.

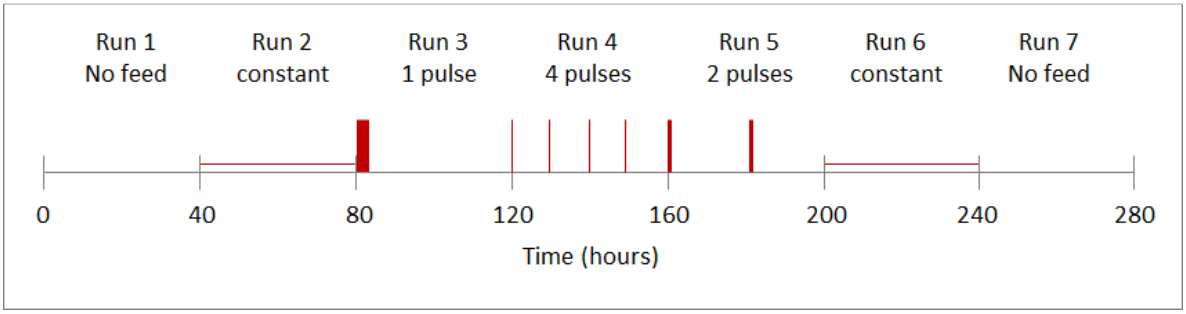


**Figure 2.2. Sequence of runs and supply regimes. Horizontal lines represent constant feed. Vertical lines represent pulses and the thickness of the line represents the size of the pulse.**

Run 1 (R1) had no feed and was conducted to develop more realistic bed surface conditions. In Run 2 (R2), 300 kg of sediment were introduced at a constant feed rate (2 g/ms) over the 40 hours. To examine the response of the system to a large supply episode, in Run 3 (R3) the 300 kg of material was dumped in just one big pulse at the beginning of the run. During Run 4 (R4), the 300 kg of sediment was divided in four 75 kg pulses that entered the flume every ten hours. To produce supply conditions in between those of R3 and R4, in Run 5 (R5) the same material was divided in two 150 kg pulses that entered the system every 20 hours. To explore the importance of the initial bed state on transport adjustment and bed evolution, Run 6 had the same constant feed regime as R2; and Run 7 had no feed as R1. All pulses were introduced at a rate of 83 g/ms, but the feed duration was different. The 300 kg pulse lasted one hour, the 150 kg episodes lasted half an hour each, and the 75 kg inputs had duration of 15 minutes. Supply conditions at each run are presented in Table 2.1.

| Run | 1 | 2 | 3 | 4 | 5 | 6 | 7 |
|---|---|---|---|---|---|---|---|
| Supply regime | No feed | Constant | Episodic | Episodic | Episodic | Constant | No feed |
| N° of pulses | 0 | 1 | 1 | 4 | 2 | 1 | 0 |
| Feed rate (g/ms) | 0 | 2.083 | 83.33 | 83.33 | 83.33 | 2.083 | 0 |
| Feed duration (h) | 0 | 40 | 1 | 0.25 | 0.5 | 40 | 0 |

**Table 2.1. Supply conditions at each run.**

## 2.2 Data collection

During each run, data related to the flow, the bed and bedload were collected. The sequence of measurements that was followed in most runs is presented in Figure 2.3. The exceptions were R4 and R5, which required measurements more often because of the way that the sediment was introduced to the flume. In R4 the sequence of measurements from 0-10 hours was repeated after each pulse. In R5, the sequence from 0-20 hours was repeated twice. Data regarding sediment transport was collected at the downstream end of the flume. To collect data over different areas of the bed (i.e. velocity profiles, elevations, texture), a motorized cart was used (Figure 2.4).

The flow had to be reduced or increased on many occasions. This was done to change the sediment trap, scan the bed and take photos of the bed surface. It was also done each time the experiment needed to be paused. Changes in water discharge were always conducted in the same way. The flow was slowed down in a gentle way, and the bed had to be completely wet before slowly increasing the flow again.

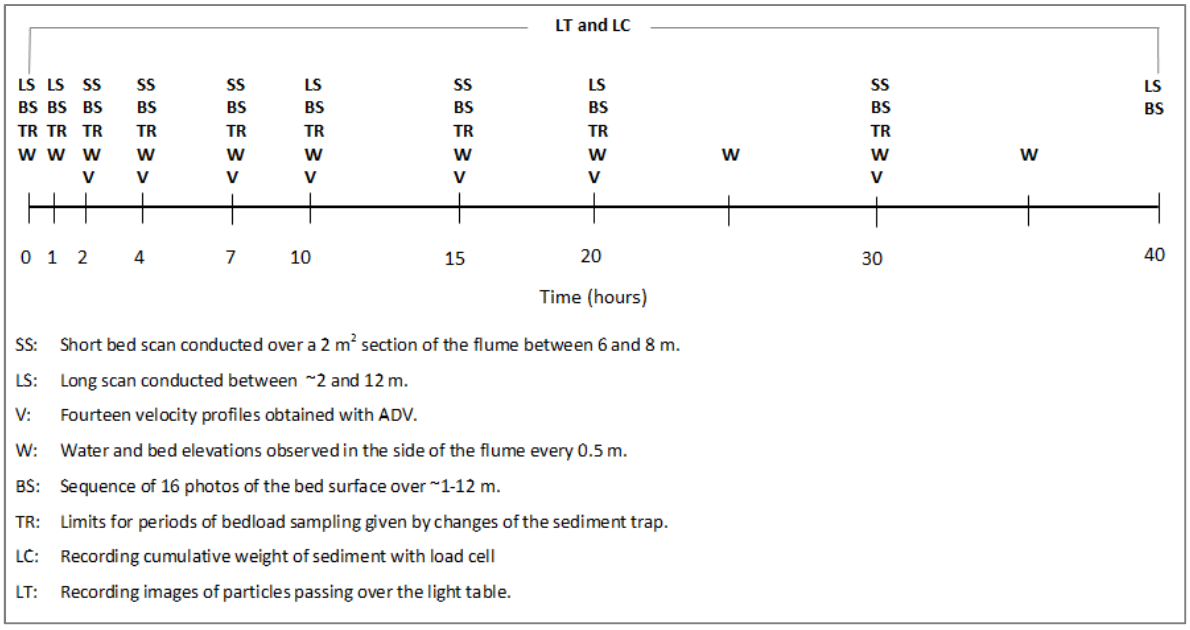


**Figure 2.3. Data collection during an experimental run. In Run 4 the sequence of measurements between 0-10 hours was repeated after each pulse. In Run 5 the sequence over 0-20 hours was repeated twice. Transport data was recorded continuously with the load cell and light table methods.**

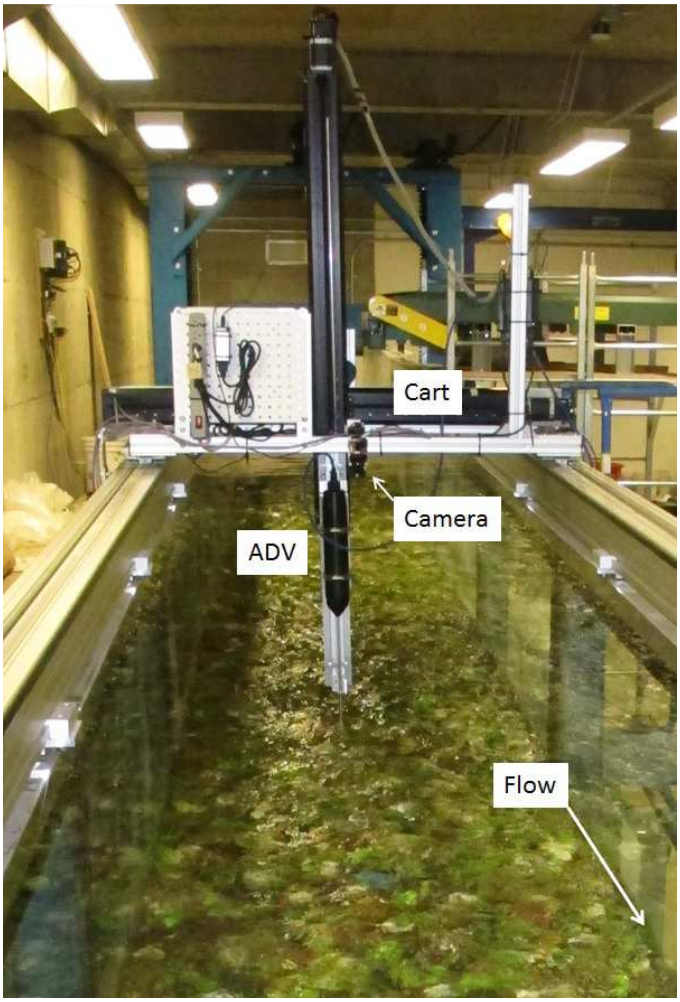


**Figure 2.4. Motorized cart used for data collection along the flume. In the picture, the ADV (acoustic Doppler Velocimeter) used to get velocity profiles and the camera used in bed scans are mounted on the cart.**

### 2.2.1 Flow characteristics

Even though water discharge was set constant at 65 L/s during the experiment; water elevation and water depth were measured every one to five hours to characterize the flow. Plastic rulers were placed every 0.5 m on one side of the flume to visually estimate the three maximum and three minimum values of water elevation over one minute periods (Figure 2.5). These values were used to estimate representative averages of water elevation to obtain water surface slopes. Bed elevation was indicated at the same points to estimate water depth by subtracting bed elevations from water elevations. Mean depths along the flume and mean surface slopes were used for shear stress estimations.

To estimate water velocities in three dimensions and observe variations in the flow field due to changes on the bed surface composition, fourteen water velocity profiles were recorded using the

Nortek Vectrino II Acoustic Doppler Velocimeter (ADV). The Vectrino II gives up to 3 cm velocity profiles with a 1 mm cell resolution. Profiles were recorded for three minutes towards the center of the flume, spaced 10 cm from each other at several times during the experiment (Figure 2.3). Often, the flow was not deep enough to get a good signal because of a large particle sitting below the ADV. These results are not presented in this thesis.


**Figure 2.5. Plastic rulers on the sidewall of the flume used to observe bed and water elevations.**

### 2.2.2 Sediment transport

Sediment transport was measured at the downstream end of the flume with three different methods: video camera-light table, load cell and a sediment trap (Figure 2.6). In the first method, a high resolution video camera captured images of particles passing over a light table at a rate of 27-32 frames per second. Recorded images (.tiff) were analyzed in Labview software that provided output files (.txt) with transport data in grams and number of grains per second for each of the fourteen grain size classes that composed the sediment mixture. The Labview code is designed to identify particles by subtracting the recorded images from a background image, in which only flow passes over the light table (no movement detected). It tracks grains coordinates from a calibration image and estimate particle velocities to provide rates. This method was calibrated by comparing results for individual particles with observations and getting a weight/area relation; and tested with sieved samples from the sediment trap following the methods explained in (Zimmermann et al., 2008). Paired sample T-tests between calibrated data and 15 sieved samples showed no statistically significant difference between means at all size fractions (Table 2.2). The data from the

light table was used to present results because of its higher resolution (see Chapter 5: Sediment transport.

| Grain size class mm | P-value |
|---|---|
| 0.5-0.71 | 0.096 |
| 0.71-1 | 0.072 |
| 1-1.41 | 0.08 |
| 1.41-2 | 0.097 |
| 2-2.8 | 0.68 |
| 2.8-4 | 0.69 |
| 4-5.6 | 0.36 |
| 5.6-8 | 0.17 |
| 8-11 | 0.72 |
| 11-16 | 0.81 |
| 16-22 | 0.69 |
| 22-32 | 0.16 |
| 32-45 | 0.17 |

**Table 2.2. P-values of paired sample T-tests between fractional transport from the light table and trap data. Fifteen samples were used.**


**Figure 2.6. The light table and load cell used to collect sediment transport data, situated at the downstream end of the flume.**

The second method consisted of a load cell that recorded the cumulative submerged weight of a sediment trap. The trap was hanging from the load cell at the end of the flume. To calibrate these data, a relation was established between scaled weights and the estimations done by the load cell under the same water discharge that was used in the experiment. The standard deviation of load cell estimations for a given weight was of ~ 0.5 kg. To estimate mean transport rates from the cumulative data, the procedure explained in Marr et al. (2010) was used: (1) calibrated data was filtered with a moving average window, and (2) flux was computed by subtracting filtered weights lagged in time and dividing by the lag time. A window length of 3 minutes was used in the calculations. Even though the standard error is important, trends due to changes in feed regime were clear, and the data provided by the load cell was used to examine periods where the light table data looked suspicious or was missing.

The third method consisted of weighing and sieving the material from the sediment trap at the end of the flume. The trap was changed throughout the experiment, defining sampling periods as presented in Figure 2.3. The sediment trap was essential for testing and calibrating the light table method.

### 2.2.3 Bed elevation

Bed elevations were obtained by scanning the bed, using a video camera that recorded the reflectance location of a green laser (Figure 2.7). The scanning was controlled in Labview image processing software, where the data recorded was processed and calibrated. The outputs were .txt files with 2d matrix of bed elevations relative to the floor of the flume. The scans had a 2 mm resolution in the horizontal and longitudinal directions, and a 1 mm resolution in the vertical direction. Some bed scans covered 11 $m^2$ of the bed (long scan), while others only covered 2 $m^2$ in the center of the flume (short scan). The occurrence of one or the other was previously discussed and designed systematically to allow comparisons (Figure 2.3). Elevation data were used in different analyses regarding bed evolution. The data were used in estimating bed slope in the thalweg and net changes in elevation (aggradation/degradation). The data were also used to examine the spatial pattern of these changes, the bed topogaphy at the end of each run, and the presence of bedforms. More details on how each analysis was done are provided in Chapter 6: Bed evolution

**Figure 2.7. Green laser used for bed scans.**

### 2.2.4 Bed texture

To collect information regarding bed textures, photos of the bed surface were taken every time the bed was scanned (Figure 2.3). A camera (Canon PowerShot G12) mounted on the motorized cart was used to take a sequence of 16 photos of the bed surface between ~1-12 m. Bed surface grain size distributions (GSDs) were obtained using the point count method on the photos. The method sampled a grid of 36 *14 points with a cell size of 65 mm (largest particle size) over each photo. Grains larger than 2.8 mm were recognized. Because of time issues, pebble counts on every photo were done only at hours when long scans were available. Mean grain size statistical parameters were estimated for the 16 photos, but also for the 4 photos that covered the 2 $m^2$ section where the short scans were conducted. As the results in both cases were almost the same, the 2 $m^2$ section was used to obtain GSDs at each time photos were available. These data were used to analyze the temporal adjustments of the bed surface texture and also to scale fractional transport rates for mobility analysis (further details in these analyses are provided in Chapter 5: Sediment transport. The GSDs estimated from the 16 photos were used to examine differences in texture evolution with distance along the flume and the spatial adjustment of particle size.

# Chapter 4: Flow characteristics

The following results were obtained from bed and water surface elevations measured at the side of the flume every few hours. Results for R1 are missing. Water elevations were corrected to take into account the slope of the flume. Water surface slope was estimated as a best fit slope from corrected water elevations. An average for water depth along the flume was computed during each measurement time step. Data points situated less than 2 m from the downstream end were excluded because of the influence of downstream boundary conditions (back water effects caused by flow obstruction at the end of the flume). Data points upstream of 12 m were excluded because of non-systematical measurements (during first runs those points were not measured), but also because they were too close to the feeding area.

Mean boundary shear stress was calculated using equation 3.1, where $\tau_b$ is boundary shear stress, ρ is water density (1000 kg/m$^3$), g is acceleration of gravity (9.81 m/s$^2$), $S_w$ is water surface slope, and Y is water depth.

$$\tau_b = \rho\, g S_w\, Y \qquad 3.1$$

The Shields number (τ*) was estimated using equation 3.2, where $\rho_s$ is sediment density and $D_g$ is the geometric mean grain size of the bed surface.

$$\tau^* = \frac{\tau_b}{(\rho_s - \rho) g D_g} \qquad 3.2$$

Longitudinal profiles of bed and water elevation at various time steps are presented in Figure 3.1 to characterize the flow during the experiment. As most results were similar, only profiles at the beginning and near the end of each run are presented. A mean Froude number of 0.78 was estimated by von Flotow (2013) during the experiment. The longitudinal profiles showed that the flow was not uniform. Upstream a situation of trans-critical flow was observed, given by the existence of subcritical and supercritical flow (due to changes in bed elevation). Towards downstream the curve suggests subcritical flow that close to the downstream end is affected by an increase in water depth (and consequently a reduction of water velocity) due to flow obstructions.

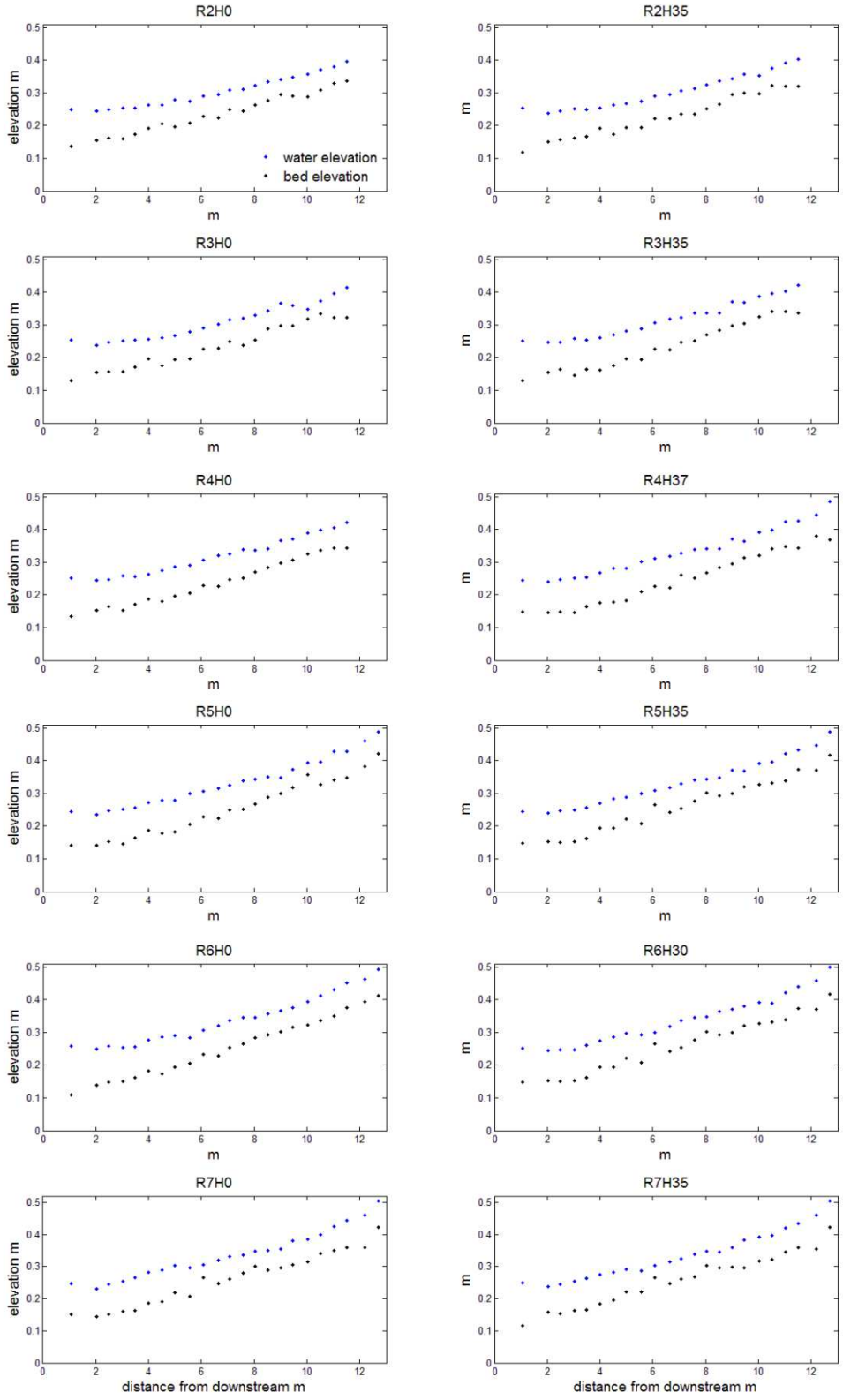


**Figure 3.1. Long profiles of water and bed elevations at different runs (R) and time in hours (H).**

Even though water discharge was set constant at 65 L/s during the experiment, flow parameters exhibited changes probably related to changes in the bed elevations and bed surface composition due to sediment supply. Mean parameters and standard deviations for each run are presented in Table 3.1.

| Run | Water depth -m | | Water surface slope - m/m | | Mean boundary shear stress - Pa | | Shields number | |
|---|---|---|---|---|---|---|---|---|
| | mean | SD | mean | SD | mean | SD | mean | SD |
| **R2** | 0.070 | 0.0031 | 0.0171 | 0.0009 | 11.66 | 1.09 | 0.051 | 0.003 |
| **R3** | 0.077 | 0.0031 | 0.0189 | 0.0004 | 14.29 | 0.71 | 0.066 | 0.013 |
| **R4** | 0.080 | 0.0015 | 0.0197 | 0.0004 | 15.57 | 0.50 | 0.070 | 0.004 |
| **R5** | 0.079 | 0.0032 | 0.0200 | 0.0006 | 15.47 | 0.93 | 0.069 | 0.004 |
| **R6** | 0.080 | 0.0046 | 0.0203 | 0.0008 | 16.03 | 1.43 | 0.072 | 0.009 |
| **R7** | 0.075 | 0.0017 | 0.0199 | 0.0002 | 14.55 | 0.38 | 0.064 | 0.004 |

**Table 3.1. Mean values and standard deviations of water depth (m), water surface slope (m/m), mean boundary shear stress (Pa), and Shields number during each run. Data for R1 is missing.**

Water surface slope varied between 0.017 and 0.021 m/m and exhibited a slight increase from R2 to R6 (Figure 3.2.a). During R7, it showed a very small decrease. Mean water depth had values between 0.07 and 0.08 (Figure 3.2.b). From R2 to R4 there was an increase in mean water depth. During R5 water depth showed considerable variations, and during R6 the flow was relatively deep during the first 20 hours, but after that water depth showed a decrease of ~1 cm. Since then, a very slow decrease was observed towards the end of the experiment. Mean boundary shear stress fluctuated between 11 and 16 Pa most of the time and showed a similar trend to water depth (Figure 3.2.c).

The critical dimensionless shear stress for entrainment is commonly approached with the Shields number. A wide range of values had been suggested in the literature, and a value close to 0.045 is considered to be appropriate for the entrainment of the $D_{50}$ on gravel beds with poorly sorted sediment like the bed used in this study. Shields numbers deviated from the 0.045 for poorly sorted sediment, and fluctuated between 0.045 and 0.09 (Figure 3.3). This is consistent with results for gravel beds showed in Parker (2007), which show a variability of Shields numbers between 0.01 and 0.1, with no large deviations from the critical value.

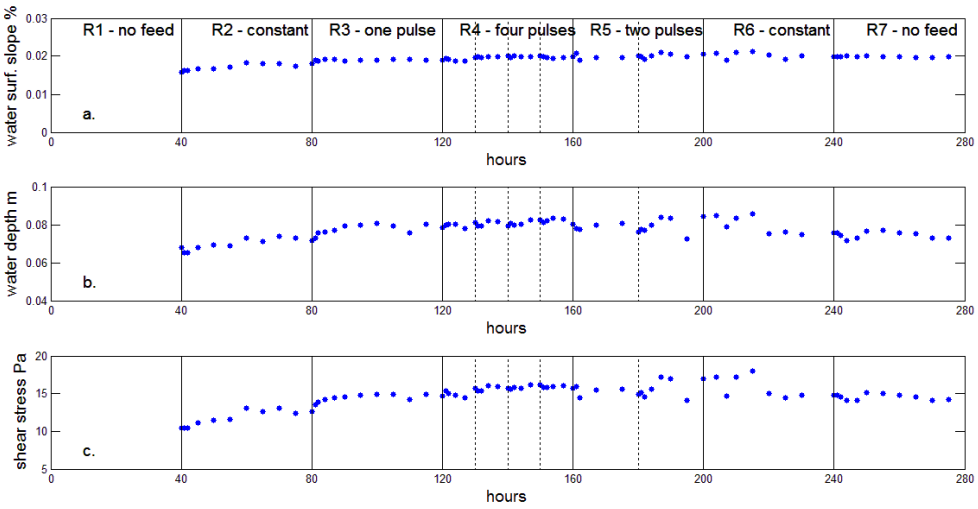


**Figure 3.2. Water surface slope (a), mean water depth (b) and mean boundary shear stress (c)**

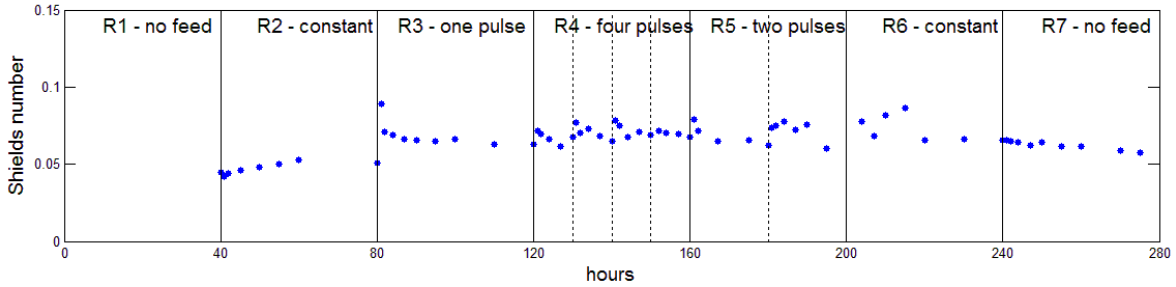


**Figure 3.3. Shields number estimated for the geometric mean of the bed surface against time.**

# Chapter 5: Sediment transport

Sediment transport data was analyzed to examine the temporal variability of the channel response to sediment supply. Three different methods were used for data collection: a sediment trap, a load cell, and a light table with a video camera (see Chapter 3: Methods for further details). Data from the light table was chosen to present results because of its higher time resolution for total and fractional transport (1 s), and because it had less noise than the data from the load cell. The latter was used to support analysis when trends in the light table were suspicious or unclear (i.e. the presence of extremely large values). To check if there was under/over sampling of any size fractions, results from the light table were compared to those obtained from the trap.

There are few periods where data is missing due to file corruption after image processing in Labview. These periods occurred between hours 15-20 in R1, and hours 10-15 in R2. Shorter periods (< one hour) are due to sudden problems in data recording, or because of large particles getting stuck in the outlet of the flume and causing bubbles that were detected as false particles. These gaps had no serious implications for data analysis and temporal patterns of sediment transport could be interpreted.

## 4.1 Transport rate time series

Temporal patterns of sediment transport rates were analyzed by looking at total transport rates, but also at fractional transport rates to get better knowledge of the behavior of grains of different sizes. Total transport rates were smoothed using a 30 second running mean and are presented in g/ms. As the intensity of movement was different for finer and coarser grains, they were analyzed in different ways. Finer grains (< 8 mm) moved constantly and in higher proportions. These sizes were divided in two groups: sand (< 2 mm) and fine gravel (2-8 mm), and their time series were smoothed in the same way as total transport rates. Grains coarser than 8 mm moved more sporadically, and could become immobile for considerable periods of time. Because of this reason a running mean was not adequate, and these fractions are presented separately in number of grains per second. Feed rates are plotted with total transport rates for comparisons.

Results for Run 1 (R1) are plotted in Figure 4.1. Total transport rates were high at the beginning of the run (~100 g/ms), and exhibited a fast decrease during the first hours. There is a gap in the data from hour 10 to 15. After hour 20, the transport rate was asymptotic around 0.2 g/ms, value that is about three orders of magnitude below initial transport rates. Bed load showed high variability.

A few peaks can be observed in the plot at about hours 10, 15, 20, 26, 30 and 35. Peaks occurred at almost regular intervals of time, in what reflects a certain pattern of behavior in sediment transport. There was an increase in transport rates during the last two hours.

Sand (< 2 mm) and fine gravel (2-8 mm) exhibited similar trends to total transport rates, and the occurrence of relatively large values was synchronized. Sand rates plotted about two orders of magnitude below fine gravel rates. This could be influenced by under sampling of finer fractions with the light table method, as shown in Figure 4.2.

The movement of coarse sediment was sporadic and less intense. Furthermore, the number of mobile grains declined significantly with particle size. There was a decrease in the intensity of movement of sizes up to 22 mm, because of bed surface structuring and armoring. The movement of grains of 8-11 mm and 11-16 mm declined during the first five or ten hours. After that, sediment transport intensity was low, and there were considerable periods of no movement, especially for grains between 11-16 mm. Grains of 16-22 mm moved sporadic and mostly during the first 10 or 12 hours. Only few grains of 22-32 mm moved during the first 15 hours, and no grains coarser than 32 mm moved during the entire run.

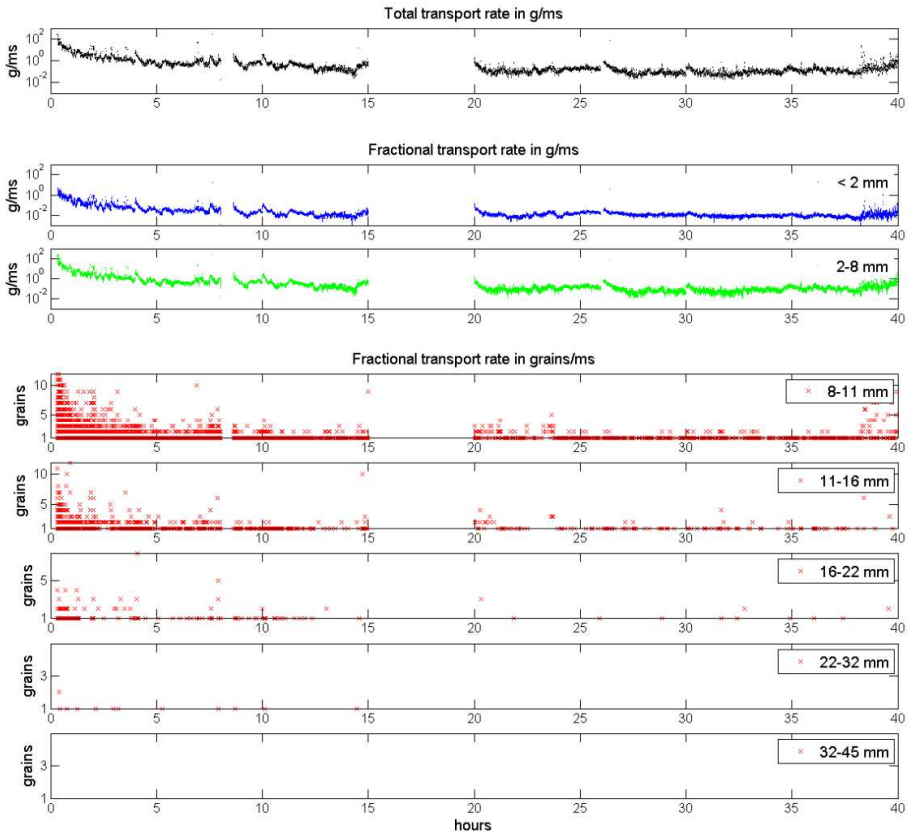


**Figure 4.1. Sediment transport rate during Run 1. This run had no feed.**

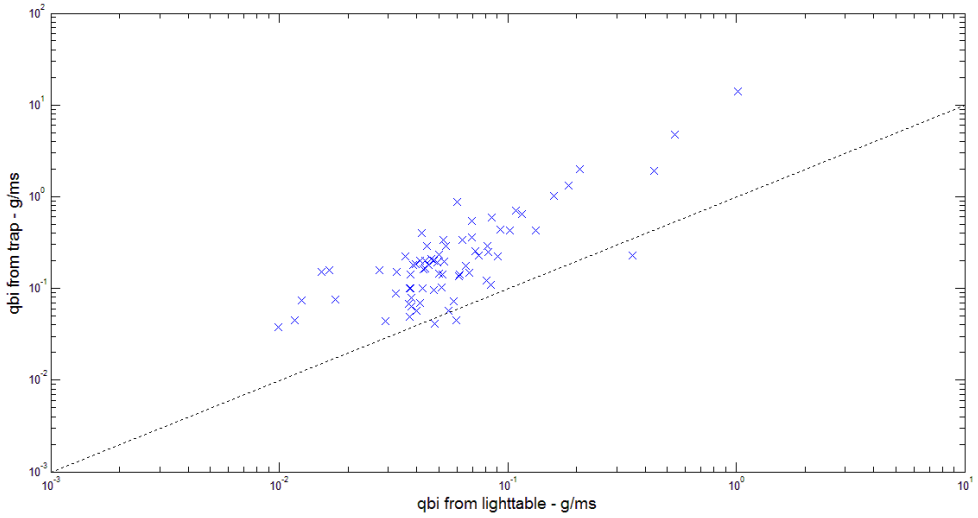


**Figure 4.2. Mean sand transport rates from the light table versus sand rates estimated from sediment trap. Dashed line represents 1:1 relation.**

Results for Run 2 (R2) are presented in Figure 4.3. This run had constant feed with a rate of 2 g/ms. During the first hours, total transport rates were low and fluctuated around a mean value of ~0.2 g/ms. There was a spike at about hour four. Near hour seven, sediment transport rates increased about one order of magnitude. After this increase, transport rates fluctuated around the same values, which were slightly above transport rates at the beginning of the run. There is a gap in the data from hour 10 to 15. Large peaks were observed at hours 20 and 30. After hour 30, there was a gradual increase in transport rates, and towards the end of the run, they approached the feed rate.

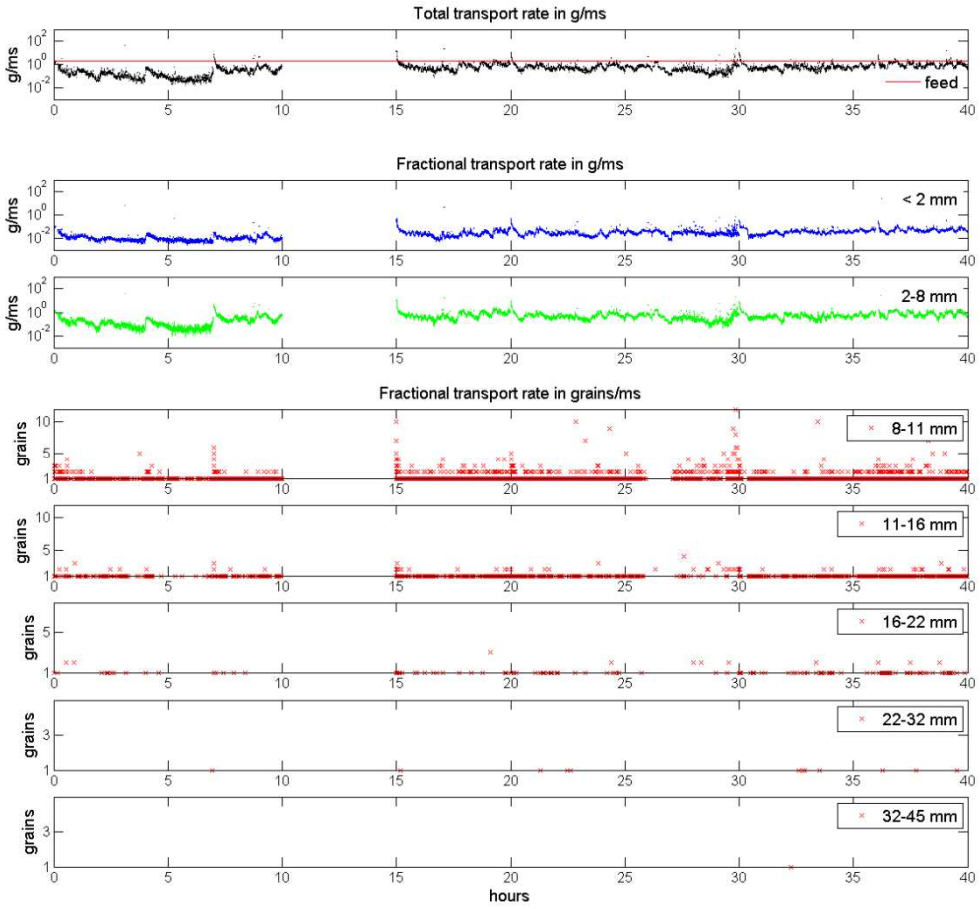


**Figure 4.3. Sediment transport rate during Run 2. This run had constant feed at 2 g/ms.**

The patterns in fractional transport rates differed with grain size. Sand (< 2 mm) and fine gravel (2-8 mm) mimic total transport rate patterns. Peaks at hours 4, 7, 20 and 30 were also identified. Transport rates of all grains > 8 mm were always sporadic and of low sediment transport intensity. Grains of 8-11 mm followed the same trend as total transport series, exhibiting small peaks at

nearly the same time. Because of the low intensity of movements it was very difficult to identify changes in the trend of grains > 11 mm. The movement of grains of 16-32 mm was insignificant (few hours with no movement), and no grains larger than 32 mm exited the flume.

Run 3 (R3) had an episodic feed regime, in which a 300 kg pulse entered the system in one hour at a feed rate of 83 g/ms (Figure 4.4).

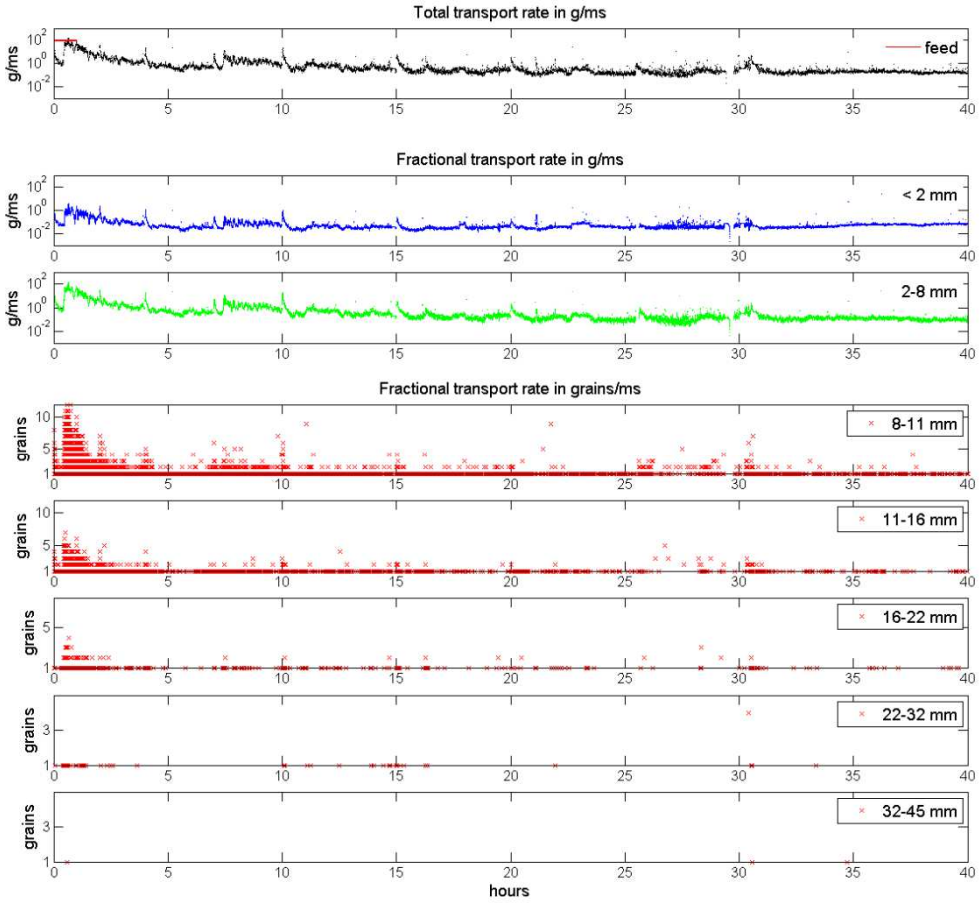


**Figure 4.4. Sediment transport rate during Run 3. In this run one 300 kg pulse entered at a rate of 83.3 g/ms during the first hour.**

Total transport rates showed a sharp increase of two orders of magnitude after half an hour, reaching similar values to the feed rate. After the largest peak, sediment transport rates decreased monotonically and had considerable short term variation. Smaller peaks were observed at hours 2, 4 and 6.5. At roughly hour seven, sediment transport rates increased suddenly by one order of magnitude. Then, transport rates started to decline, but slower than they did after the largest peak at hour 0.5. Since hour 10 or 12, the decline was more gradual. Few significant peaks were

observed at hours 10, 15, 20, 26 and 31. During the last ~seven hours, transport rate exhibited little variation and was almost constant with a mean rate close to 0.1 g/ms. This value was similar to the value obtained for the last hours of R1 (no feed), and it was below the transport rates before the pulse.

Sand and fine gravel exhibited similar trends to total transport rate, showing peaks at similar times. The largest peak occurred at hour 0.5 and it was more pronounced in fine gravel than in sand. The rate of movement of size fractions from 8 to 32 mm increased at the beginning of the run, which was consistent with the trend obtained for the total load. The intensity of movements of grains 8-16 mm was significantly higher during 0.5 – 2 hours, suggesting the passage of a 'sediment wave'. After a few hours transport intensity was low, and small peaks occurred at the same time as in total transport rates. Even though grains of 16-32 mm always moved sporadically and with low intensity, their movement is consistent with peaks observed in total transport rates. Only three grains coarser than 32 mm were registered during this run.

Results from Run 4 (R4) are presented in Figure 4.5. This run had an episodic feed regime, in which four small 75 kg pulses entered the system. Pulses were introduced every ten hours, at a rate of 83 g/ms, and lasted 15 minutes. Total transport rates exhibited similar behavior after each pulse except for the third one. After each pulse, sediment transport rates increased about one order of magnitude and then decreased towards values similar to those before the pulse. After the first pulse, sediment transport rates started increasing in less than one hour, a trend that persisted for ~1.5 hours. At about hour 2, transport rates reached values of ~10 g/ms, and after that started to decrease. Eight hours after the first pulse, transport rates varied around 0.5 g/ms. Peaks were noticed at hours 4 and 10. After the second pulse, sediment transport rates started increasing after one hour. The response was slightly slower than with the first pulse. At hour 12, transport rates started to decrease until the values remained relatively low after hour 16. During this period, peaks occurred at hours 11, 12, 14 and 17. After the third pulse, the transport rate response was smaller and slower than with previous pulses. Two hours after the pulse, there was a slight increase in transport rates, followed by gradual decrease. Peaks were observed at hours 20, 21, 22, and 24. After hour 25, the rates varied around the similar values, exhibiting a relatively large peak at about hour 27, and a relatively small peak at hour 30. After the last pulse, a response in transport rates is clear. About one hour after the fourth pulse, transport rates increased significantly in almost two orders of magnitude. There was a large peak at hour 31 of more than 10

g/ms. After this peak, transport rates remained relatively high for an hour or so and then gradually decrease. During this period peaks were noticed at hours 31, 32, 34 and 37.

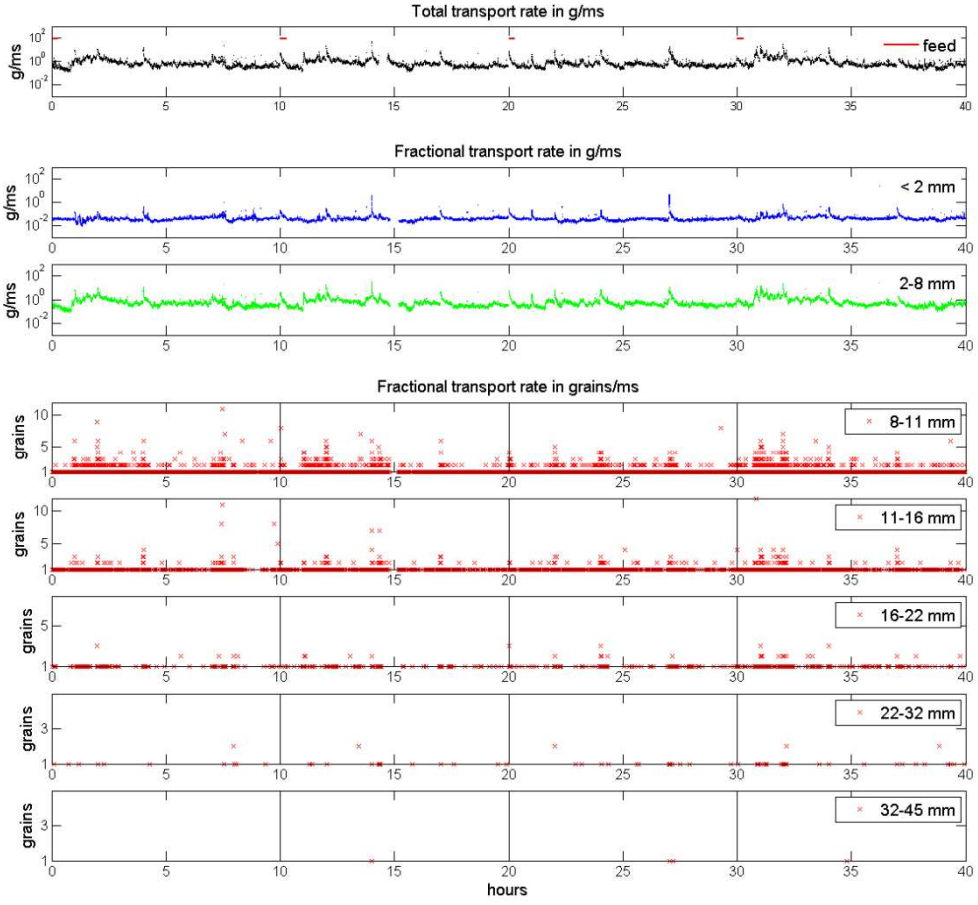


**Figure 4.5. Sediment transport rate during Run 4. In this run four 75 kg pulses entered every ten hours.**

Sand transport rates didn't increase significantly after each sediment pulse as total transport rates did. Only after the last pulse there was a small but clear increase between hours 31-34. Despite the latter, most of the peaks observed in total transport rates were also observed for sand. Fine gravels showed the same trend as total transport rates. There was an increase 1 or 2 hours after each pulse followed by decrease, and peaks were synchronized. Even though transport intensity of grains of 8-11 mm was low, there was a small increase after each pulse except for the third one. Grains coarser than 11 mm moved sporadically and with very low intensity. Because of the latter no significant changes related to the sediment inputs were identified. Few grains of 22-32 mm moved, and only four grains of 32-45 mm exited the flume during this run.

Results from Run 5 (R5) are presented in Figure 4.6. In this run, two 150 kg pulses entered the system at a feed rate of 83 g/ms. The first pulse entered at hour 0 and the second was introduced at hour 20. Feed duration was half an hour for each pulse. Total transport rates exhibited a clear response to both pulses as they did with the large pulse of R3. Thirty minutes after each pulse, sediment transport rates increase rapidly by nearly two orders of magnitudes, reaching values of ~70 g/ms. Both large peaks were followed by monotonic decay in sediment transport rates; and ten to twelve hours after each pulse, values were nearly constant at a low rate of ~0.2 g/ms. Besides the two largest peaks, smaller peaks were observed at hours 4, 7, 10, 12.5, 14, 15, 20, 24, 27, 30 and 35.

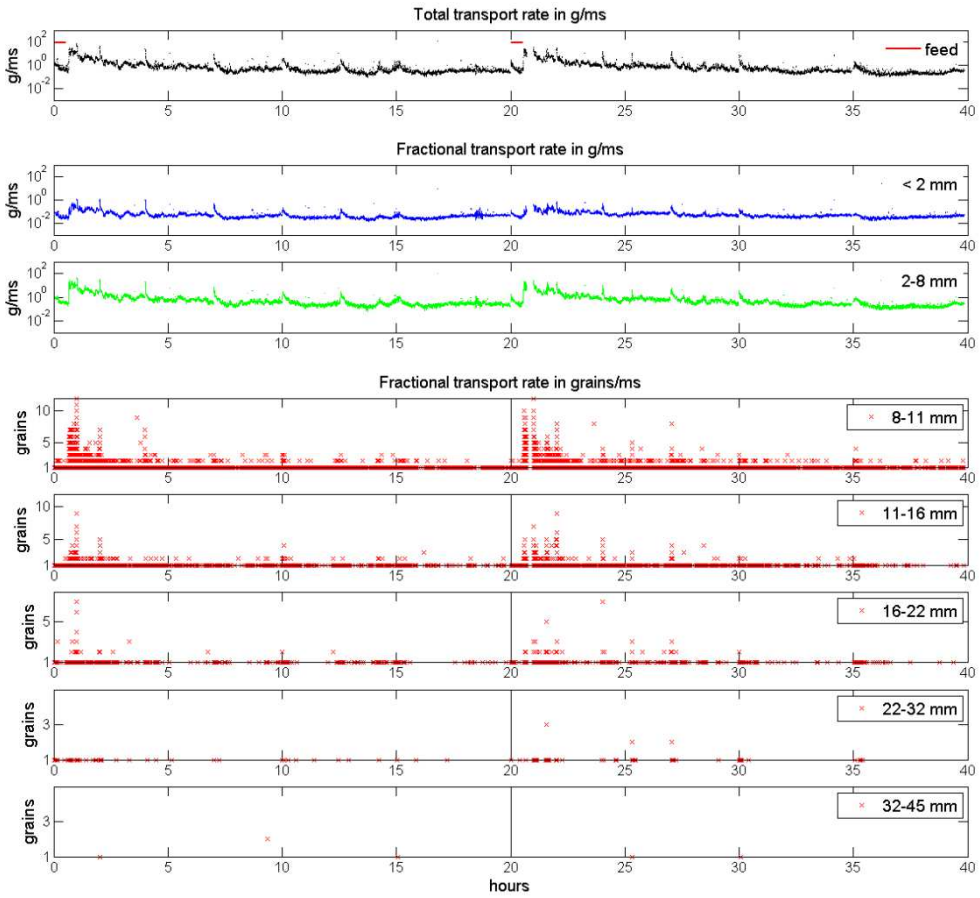


**Figure 4.6. Sediment transport rate during Run 5. In this run two 150 kg pulses entered every 20 hours.**

Sand and fine gravels showed the same trends as total transport rates: clear response to feed and synchronicity of the occasional large values. Grains of 8-11 mm showed a significant increase in transport intensity half an hour after each pulse. After one or two hours, the movement became

sporadic and uniform with low transport intensity. Grains coarser than 11 mm moved occasionally and at a very low intensity. Grains up to 22 mm exhibited a slight response to each sediment pulse. Very few grains of 22-32 mm moved, and only four grains coarser than 32 mm were tracked during the entire run.

Run 6 had constant feed at a rate of 2 g/ms (Figure 4.7). Total transport rates were below the feed rate and fluctuated around 0.1 g/ms during the first seven or eight hours. By this time, transport rates exhibited a slight increase and started to show more short term variation. There were relatively small peaks at hours 2, 10, 16, 20 and 26. The peak at hour 20 was suspicious because it plotted close to 1000 g/ms (too large). Load cell data presented a peak at this time, but it was close to 10 g/ms, which is a more realistic value. Towards the end of the run transport rates were variable around ~1 g/ms, occasionally passing the feed rate.

Sand and fine gravel rates behaved very similar to total transport rates. There was an increase in transport rates at about hour seven as a response to the feed. This response was also noted in grains of 8-11 mm. The movement of grains of 11-22 mm was uniform with low intensity during the entire run. Only few grains coarser than 22 mm moved during this run, from which only two were coarser than 32 mm.

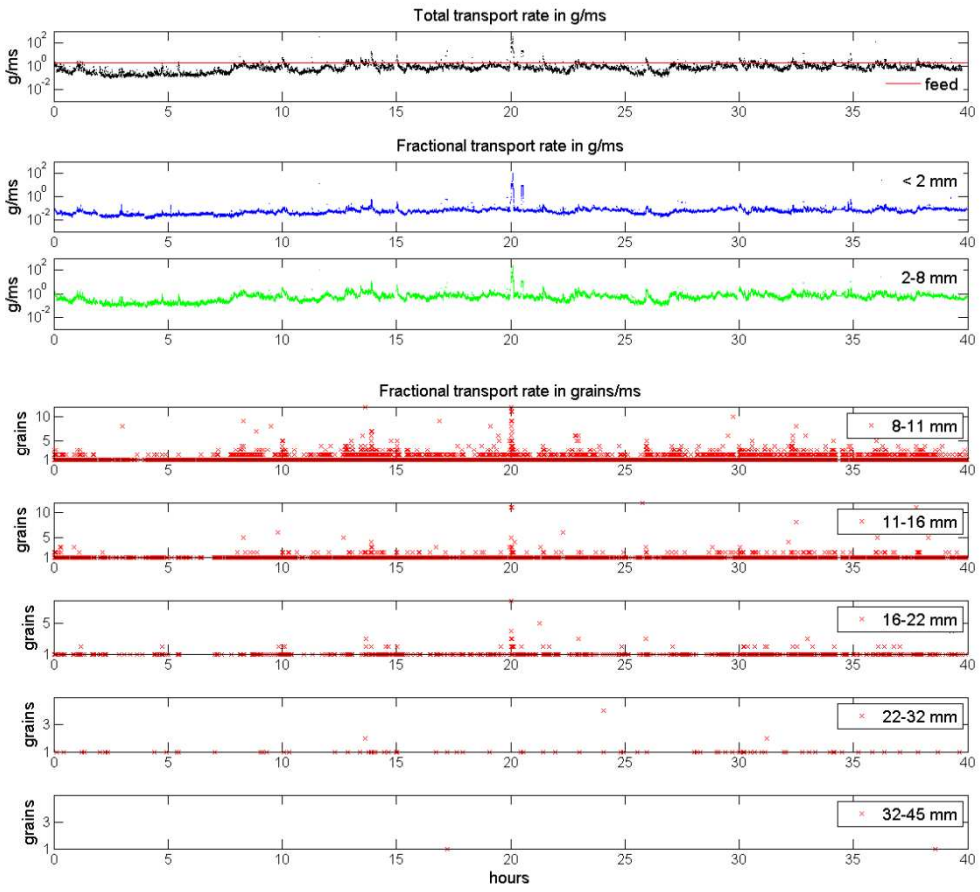


**Figure 4.7. Sediment transport rate during Run 6. This run had constant feed at 2 g/ms.**

Results from R7 are presented in Figure 4.8. During the first four hours, total transport rates exhibited a complex pattern. There were extremely large values at hour 3 (~1000 g/ms) that could be errors because they were not present in load cell data. Since hour 5, transport rates varied around ~0.3 g/ms. Distinctive peaks were observed at hours 4, 7, 10, 15, 20 and 28. Towards the end of the run peaks were smaller and occurred less frequently. Though it was difficult to see, a decrease in transport was suggested when values at the end of R7 were compared to those towards the end of R6 (0.3 and 1 g/ms respectively). This idea was supported by time series from the load cell that showed a slow decrease in transport rates until hour 10, and after that a more uniform trend. Sand and fine gravels showed the same behavior as total transport rates. Grains coarser than 8 mm moved with low intensity and only few grains coarser than 22 mm moved during this run.

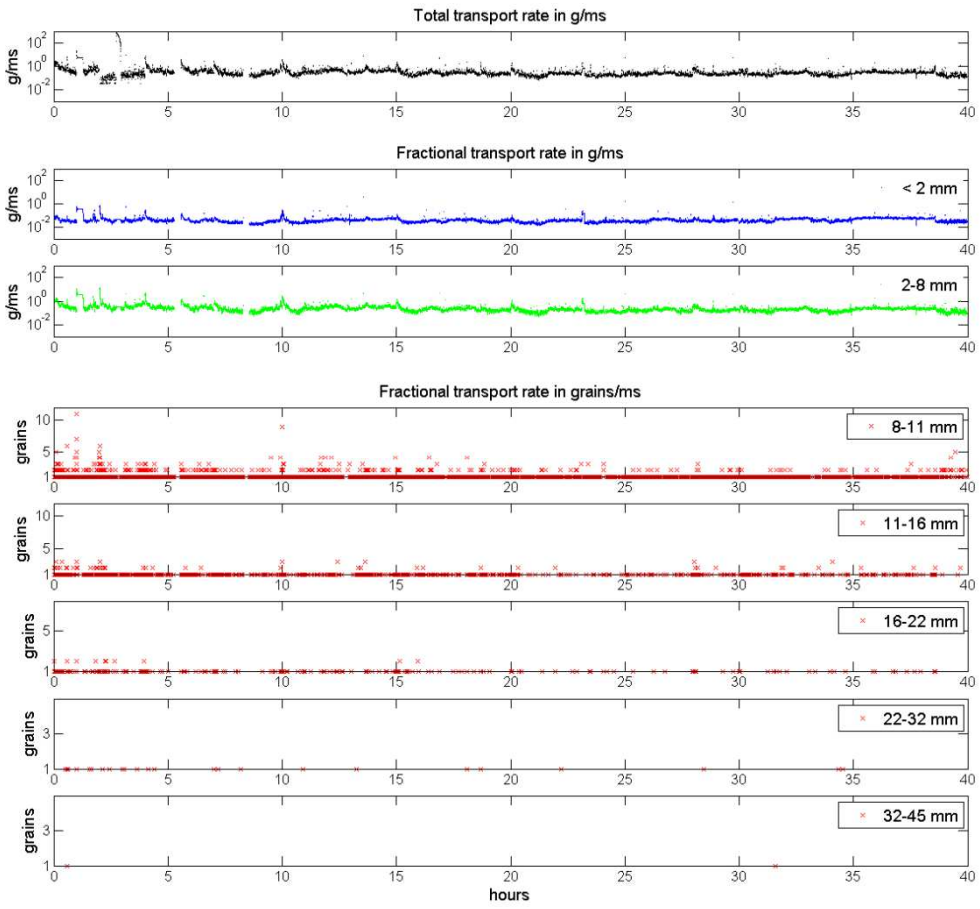


**Figure 4.8. Sediment transport rate during Run 7. This run had no feed.**

## 4.2 Particle size adjustment

To examine the temporal adjustments on the texture of the bedload and bed surface in response to changes in sediment supply, statistical parameters were estimated. The geometric mean ($D_g$), the grain size at which 90 % of the material is finer ($D_{90}$), and the grain size at which 16 % of the material is finer ($D_{16}$) were computed over one hour periods for the bedload. One hour was enough time to get rid of fluctuations due to errors, but long enough to keep variability and identify changes in the trend. Grain size parameters for the bed surface were estimated each time photos were available, using GSDs obtained from a $2m^2$ area of the bed between ~6-8 m from downstream (see section 2.2.4 for more details). This area was sampled with higher temporal resolution than the rest of the bed, and it showed similar results to GSDs estimated over the entire flume (Figure 4.9). The latter were used to analyze spatial patterns of bed surface texture (in the longitudinal direction).

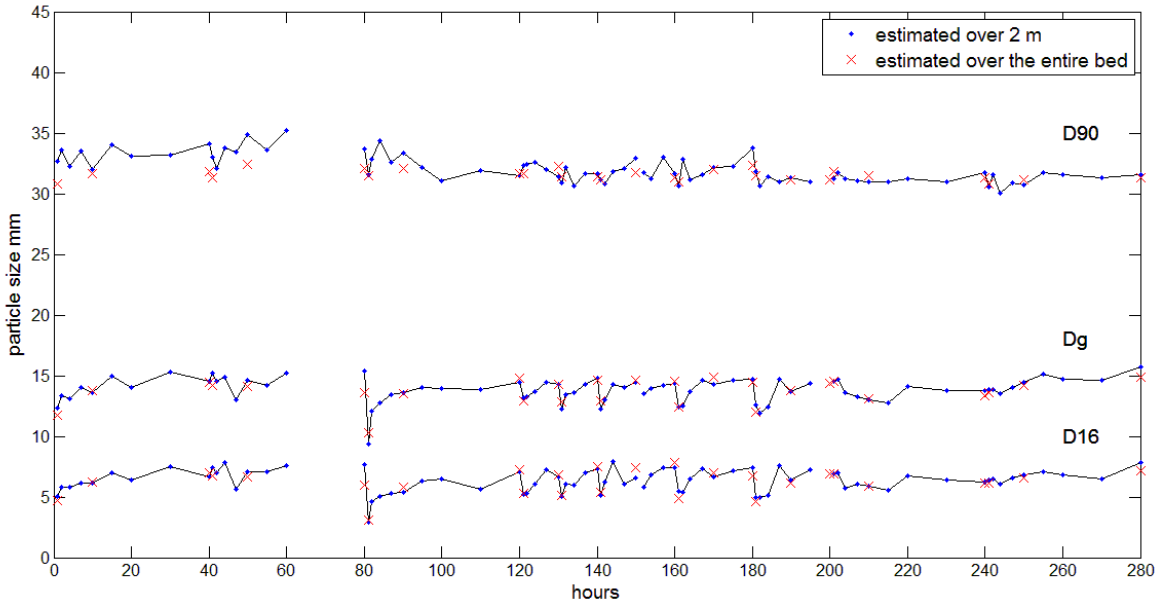


**Figure 4.9. Grain size statistical parameters of the bed surface estimated over the entire flume and over a $2m^2$ area between 6 and 8 m from downstream.**

The geometric mean ($D_g$), $D_{16}$ and $D_{90}$ of the bedload and bed surface are plotted against time in Figure 4.10. For comparisons, values for the feed material are also displayed. Mean statistical parameters and their standard deviation over the entire experiment are presented in Table 4.1.

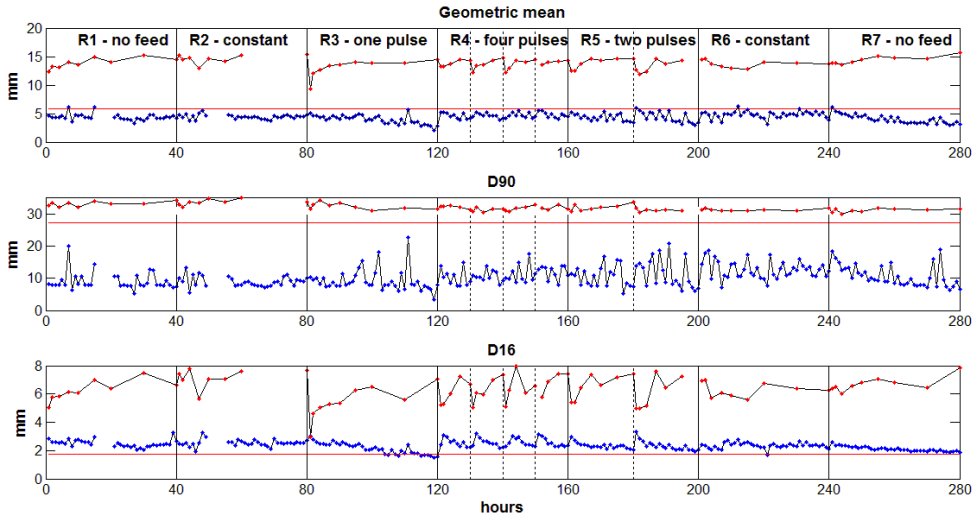


**Figure 4.10. Geometric mean, D90 and D16 of bedload (blue dots), bed surface (red dots) and feed material (horizontal line) against time.**

| | Bedload | | | Bed surface | | |
|---|---|---|---|---|---|---|
| | $D_{16}$ | $D_g$ | $D_{90}$ | $D_{16}$ | $D_g$ | $D_{90}$ |
| **Mean** | 2.4 | 4.4 | 10.4 | 6.4 | 13.8 | 32.1 |
| **Standard deviation** | 0.3 | 0.7 | 3.2 | 0.9 | 1 | 1.1 |
| **Maximum size** | 3.4 | 6.4 | 22.6 | 8 | 15.7 | 35.2 |
| **Minimum size** | 1.5 | 2.1 | 3.4 | 2.9 | 9.4 | 30 |

**Table 4.1. Mean value, standard deviation, and maximum and minimum size of grain size statistical parameters during the experiment. All values are in mm.**

The evolution of the bed surface texture during each run was conditioned by the final texture of the previous run, feed texture and flow competence. Bedload textures were conditioned by the evolution of the bed surface and flow competence. In general, the texture of the bed surface was coarser than the bedload and feed. The $D_g$ and $D_{16}$ of the bed surface varied over a wider range of sizes than $D_g$ and $D_{16}$ of the bedload. The opposite happened with the $D_{90}$ that covered a relatively narrow range of sizes for the surface and a wide range of sizes for the bedload. The $D_g$ of the bedload fluctuated around a mean of 4.4 mm, which was smaller than $D_g$ of the feed material (5.7 mm), and considerably finer than the $D_g$ of the surface, in which the mean values were 13.8 mm. Changes in the $D_g$ were primarily caused by changes in supply, and were more pronounced for the surface than the bedload.

The $D_{90}$ of the bedload oscillated between 3.4 and 23 mm, with a mean of 10.4 mm (slightly below the mean $D_g$ of the surface). It was significantly finer than the $D_{90}$ of the feed and the surface. The short term variation reflected the sporadic nature of the transport of coarse fractions. Fractional transport rates revealed that grains coarser than 11 mm could become immobile for considerable periods of time, so large values in the $D_{90}$ could be related to the movement of coarse grains. The $D_{90}$ of the bed surface was coarser than the feed. The $D_{16}$ exhibited clear responses to changes in sediment supply. The $D_{16}$ of the bedload oscillated between 1.5 and 3.4 mm. It could be overestimated because of under sampling of fine material with the light table (Figure 4.2). It was always coarser than $D_{16}$ of the feed (1.7 mm) and usually finer than $D_{16}$ of the surface, except at hour 81 (one hour after the large pulse of R3). In general, the $D_{16}$ of the surface was coarser than the $D_g$ of the bedload.

During R1 when there was no sediment feed, $D_g$ of the bedload was fluctuating and always below $D_g$ of the feed, whereas $D_g$ of the surface coarsened. The initial parameters were the same for the mixture and the surface because of the well mixed bed. Significant coarsening occurred in the $D_g$ of the surface during the first hours. After that, little changes were observed and the value was always close to 14.5 mm. The $D_{90}$ of the bedload was fluctuating, while the $D_{90}$ of the surface exhibited slow coarsening. The $D_{16}$ of the bedload got finer slowly until hour 30, whereas the $D_{16}$ of the surface coarsened during this run.

During R2 data of the surface was missing at hour 70. All bedload parameters showed significant variability; a similar behavior to R1. In R3, after the large sediment pulse there were no abrupt changes in the $D_g$ of the bedload, which only showed gradual fining over the run. The $D_g$ of the bed surface instead exhibited a clear response to the pulse. It got considerably finer one hour after the pulse, and then it started coarsening. The coarsening was faster at the beginning of the run, but after five or six hours it was very slow. The $D_{16}$ exhibited similar trends to the $D_g$. It showed gradual fining for bedload, but important changes for the surface in response to the feed. Regardless of short term variations, the $D_{90}$ of the bedload showed a slight fining trend during this run. The $D_{90}$ of the surface didn't show major changes.

In R4, the $D_g$ of the bedload coarsened significantly after the first pulse, reaching a value close to the $D_g$ of the feed. Then, it exhibited gentle fining until the next pulse entered the system. After the second pulse, a similar trend was observed, though initial coarsening was less pronounced. The response to the third pulse was not clear, and $D_g$ exhibited regular spikes. After the last pulse,

the behavior was the same as with the first two pulses. The response of the $D_g$ of the surface to sediment supply was clear. One hour after each sediment input started, the bed surface got considerably finer and then coarsened until reaching a value similar to that before the pulse. The $D_{90}$ of the bedload was variable, but it didn't change accordingly to the feed. The $D_{90}$ of the surface showed little changes. The $D_{16}$ of the bedload coarsened during the first few hours after each pulse, and then it got finer until a new pulse entered the system. The $D_{16}$ of the surface showed opposite trends. It got finer just after each pulse and then coarsened.

There was no significant response in the $D_g$ of the bedload to the first sediment input in R5. It got smaller gradually during ~20 hours. One hour after the second pulse entered the system at hour 180, the $D_g$ had coarsened ~3 mm. Just after that, it became smaller, reaching values similar to those before the pulse at the end of the run. The $D_g$ of the surface got finer during the first two hours after each pulse and then it exhibited monotonic coarsening. There was no clear response of $D_{90}$ to supply. The $D_{90}$ of the bedload had large variability. The $D_{90}$ of the surface slightly coarsened after the first pulse. After the second one, it first got finer, and then showed nearly constant values. The $D_{16}$ showed the same response to supply as it did in R4. For the bedload, it coarsened immediately after each pulse and then got finer. For the surface, it got finer just after each pulse, and then it coarsened.

During R6, the $D_g$ of the bedload fluctuated around a mean of 4.8 mm. The $D_g$ of the surface got finer during the first 15 hours. At hour 20 it slightly coarsened and no important changes were observed during the rest of the run. The $D_{90}$ of the bedload coarsened relative to its values at the end of the previous run, whereas the $D_{90}$ of the surface was almost constant. The $D_{16}$ of the bedload during the first hours showed similar values to those at the end of R5. At hour eight, it slightly coarsened, and since then it fluctuated around 2.4 mm. The $D_{16}$ of the surface became smaller during the first 15 hours and then it coarsened. All bedload parameters got finer after the feed was stopped at the beginning of R7. The bed surface tended to coarsen instead. This is better appreciated in the $D_g$ and $D_{16}$ because $D_{90}$ was nearly constant.

Even though mean statistical parameters estimated over the entire bed showed similar results as those estimated over the 2 $m^2$ section, bed surface texture was diverse along the flume (Figure 4.11).To examine this diversity and the spatial adjustments of particle size in the longitudinal direction, temporal changes of grain size parameters were analyzed at different positions of the

flume. Spatial segregation in other directions was observed (as shown in Figure 4.12), but is not presented.

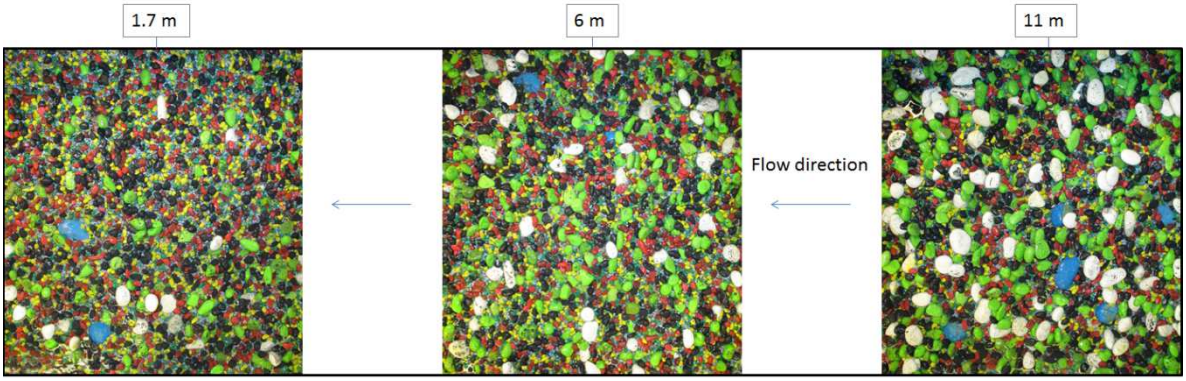


**Figure 4.11. Bed surface at the end of the experiment (R7H40). The bed texture changed with distance from downstream, being significantly coarser upstream (downstream fining trend).**

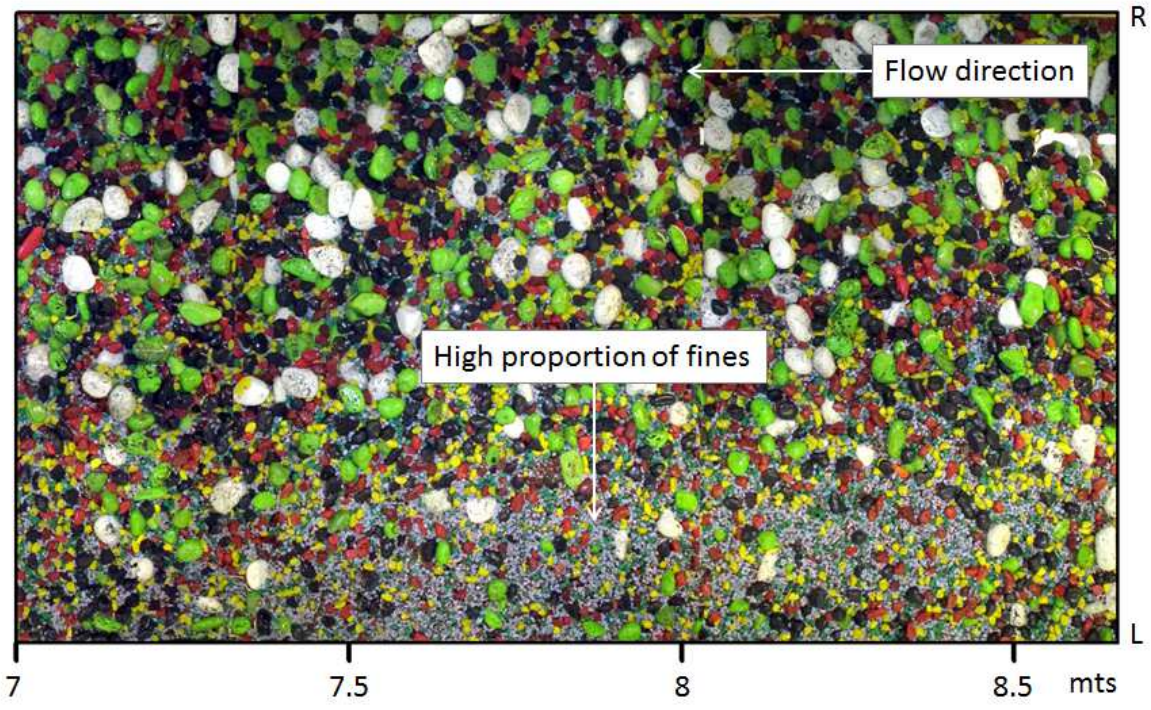


**Figure 4.12. Spatial grain size segregation at the end of Run. There is a large amount of fine material towards the left side of the flume, suggesting the presence of a fine patch.**

The evolution of $D_{16}$, $D_g$, $D_{90}$ and geometric standard deviation at three different locations (at 4 m, at 7 m, and at 10 m from the downstream end) are presented in Figure 4.13. In most cases, the parameters showed the largest values upstream (at 10 m) and the smallest downstream (at 4 m), insinuating general downstream fining. The $D_g$ showed that the bed was always armored and that

armor ratios changed with distance downstream because of the downstream fining (Figure 4.13b and Table 4.2).

The $D_{90}$ revealed important differences at each position (Figure 4.13c). Downstream (at 4 m) it exhibited less variation than in the other positions, and it was similar to the $D_{90}$ of the bulk. The geometric standard deviation at all locations was always smaller than the standard deviation of the bulk and fluctuated between 2 and 2.5 (Figure 4.13d). There was no relation between its value and the position in the flume, but it showed a small increase in response to sediment inputs.

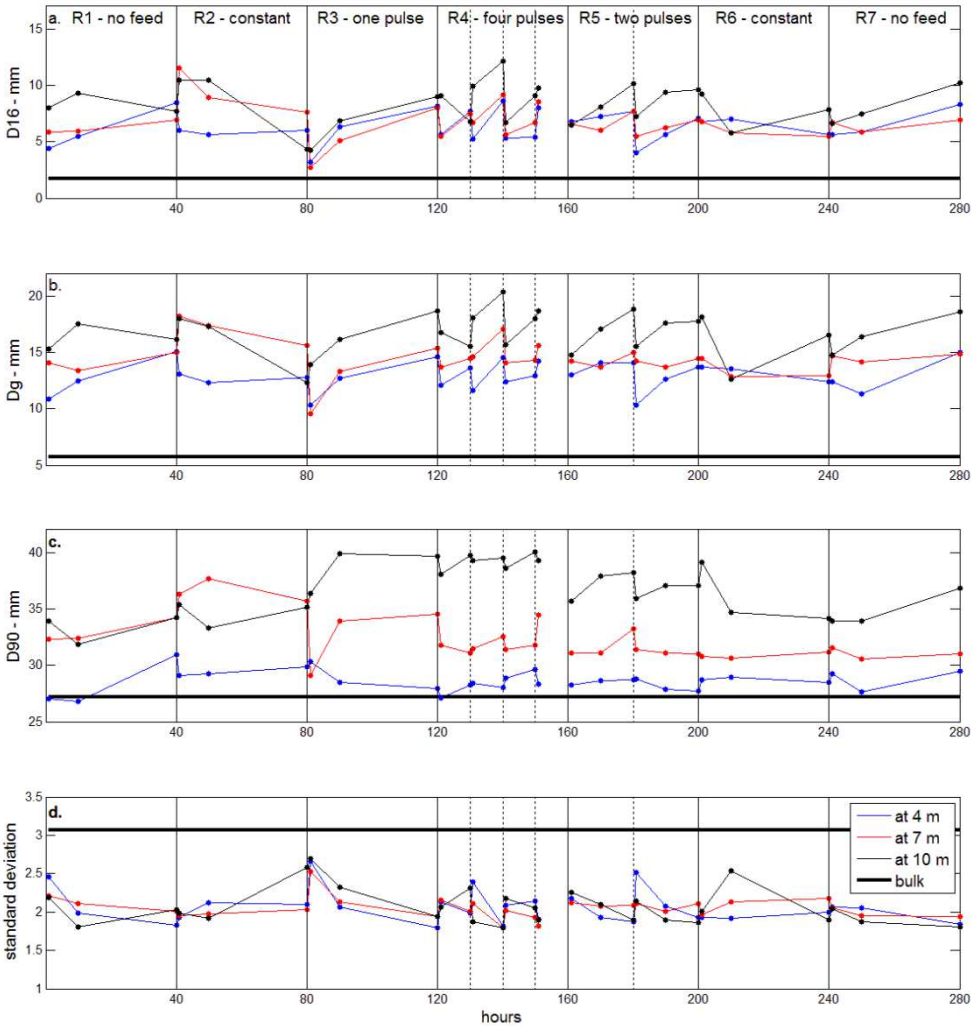


**Figure 4.13. Evolution of grain size statistical parameters of the bed surface at three different locations. D16 (a), geometric mean Dg (b), D90 (c) and geometric standard deviation (d).**

| Distance from downstream (m) | Mean | Min | Max |
|---|---|---|---|
| **4** | 2.3 | 1.8 | 2.6 |
| **7** | 2.5 | 1.7 | 3.2 |
| **10** | 2.9 | 2.2 | 3.6 |

**Table 4.2. Statistics of armor ratios during the experiment at three different locations of the bed.**

## 4.3 Relative mobility of sediment

To examine if there were changes in the relative mobility of grains of different sizes due to changes in sediment supply regime, scaled fractional transport rates were analyzed. Scaling fractional rates allow comparing the movement of different sizes relative to their availability in the bed and defining a limit between fully mobilized transport and partial transport regimes. Wilcock & McArdell (1993) defined this limit as the largest size at which the proportion in transport (Pi) was about its proportion in the bed (Fi or fi). Graphically, it was identified by an inflection in the trend of scaled fractional transport rates plotted against grain size. Grains smaller than the size at the inflection point show a horizontal trend and are considered fully mobile. For coarser fractions, the trend is declining (negative slope). Fractional transport rate decreases as grain size increases, and these fractions are considered partially mobile.

The data collected during the experiment allowed scaled fractional transport rates to be analyzed in four different ways: light table data scaled by the bed surface, light table data scaled by the bulk, trap data scaled by the surface, and trap data scaled by the bulk. The same GSDs of the bed surface that were used for grain size statistics were used for scaling. All rates are presented in g/ms and represent mean values for periods of different duration given by trap data time resolution (Figure 2.3). Results for R1 using each method are presented in Figure 4.14 for comparisons. When scaled by the bed surface, results from the light table and trap show the same trend (Figure 4.14.a and c). There is a relatively steep line with negative slope (fractional transport rate decreases as grain size increases), and no evident inflection point. This situation could be due to the truncation of the bed surface grain size distribution at 2.8 mm (limits identifying finer grains on the photos).

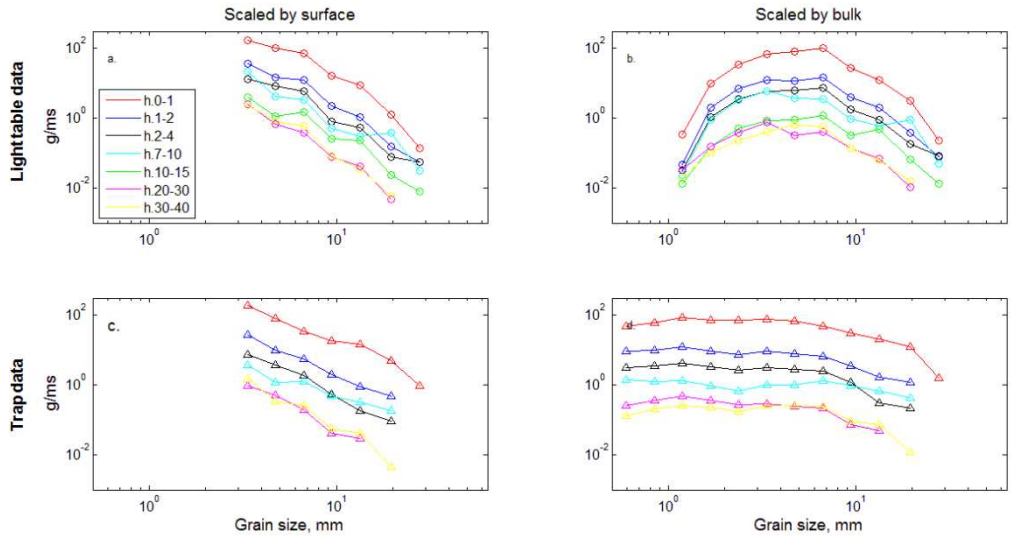


**Figure 4.14. Mean scaled fractional transport rates in Run 1 plotted against grain size. Fractional rates from the light table scaled by bed surface (a), fractional rates from the light table scaled by de bulk (b), fractional rates from the trap scaled by the bed surface (c), and fractional rates from the trap scaled by the bulk (d).**

Scaling by the bulk allows the inclusion of finer fractions and identification of inflection points. Bulk scaled fractional rates from the light table showed two inflection points: one in the fine fractions at ~1.7 mm, and the second in the coarse fractions at ~6.7 mm (Figure 4.14b). For particles finer than 1.7 mm, the fractional transport rate declined significantly, indicating an underrepresentation in fractional transport rates of these sizes. The trap data yielded a horizontal line, indicating that these sizes were fully mobile. Therefore, the underrepresentation of these sizes in the light table was due to low detection of finer fractions as supported by Figure 4.2. The second inflection point can be related to the limit between full mobility and partial transport. Particles larger than 6.7 mm showed a declining trend in which transport rates decreased as sediment size increases. This suggests that grains > 6.7 mm were partially mobile through the run, implying full mobility for particles < 6.7 mm. The inflection point in the coarse fractions was not clear in trap data (Figure 4.14d). Regardless of the method that is used, no significant change in the relative mobility of sediment was observed during R1. There was a systematic decline in the fractional transport rate due to the decline in the transport rate, but the relative proportion of each fraction in movement remained about the same. The same analysis was done for the rest, but results are not presented because they showed the same trends.

Finally, light table data scaled by grain size proportions of the bulk material was chosen to explore temporal patterns of relative mobility during the entire experiment. The bulk was chosen because

it allowed computing smaller sizes, but also because of the difficulty of matching bed surface observations with transport measurements. Results are presented in Figure 4.15, which summarizes changes in the relative mobility during the seven runs. The analysis was done for one hour periods over the entire experiment, but as the trends were similar, only results at specific times for each run are presented. For most of the runs, scaled fractional transport rates at hours 1, 10 and 40 are plotted. In R1, hour 38 was plotted instead, because of a questionable increase in total transport rates towards the end of the run (Figure 4.1). In the case of R4, as small pulses of sediment entered every ten hours, results are plotted at one and ten hours after each input. For R5, as two pulses were fed, results are given at one, ten and twenty hours after each pulse.

Transport rates behaved differently during each run, but the trends in relative mobility are very similar (Figure 4.15). R1 and R3 exhibit the same patterns, with high variability in transport rates, which spanned more than two orders of magnitude. Transport rates showed a significant decrease during R1 which was more pronounced between hours 1 and 10. There was a clear inflection in the coarse fractions at ~6.7 mm in all the cases. During R3 fractional rates showed the same inflection as R1 at hour 1 and 10, but at hour 40, the inflection in the coarse fractions was not clear.

R2 and R6 received constant feed, and showed very little variation in total transport rates. R2 showed a small increase of total transport (less than one order of magnitude). Again, there was an inflection point at ~6.7 mm at all times. In R6, there was a slight increase in transport rates of most size fractions between hours 1 and 10, but between hours 10 and 40, no increase was observed. This could be due to short term variation, as it was shown in (Figure 4.7). There was also an inflection in the trend at 6.7 mm, but it was less clear (especially at hour 40).

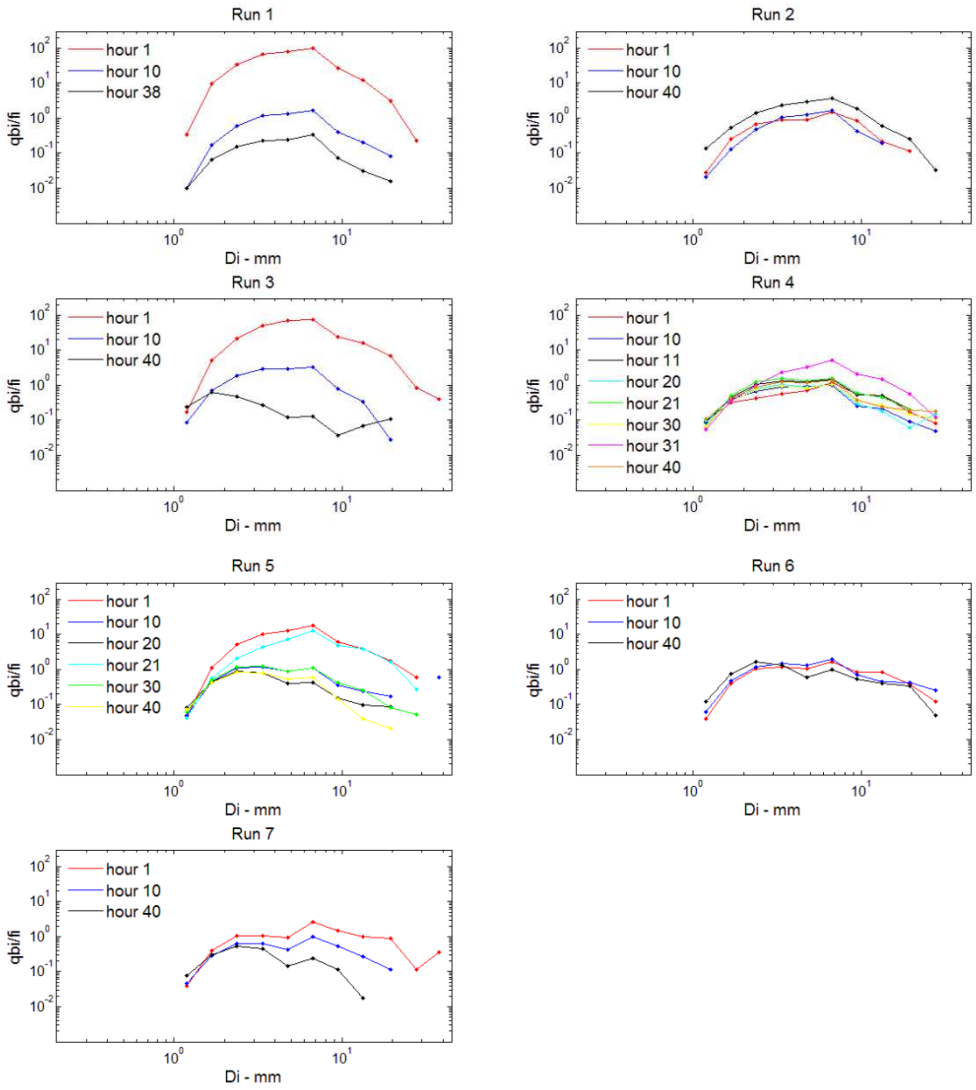


**Figure 4.15. Bulk scaled fractional transport rates (g/ms) from light table data against grain size Di (mm), at different hours of each run. Results at each time represent mean values over one hour periods. The specified time corresponds to the time at the end of each period.**

Results for R4 were very similar to those of runs with constant feed. There was no significant variation in sediment transport rates, except for hour 31, which plotted considerably higher than the others. This occurred right after the last pulse, which produced a larger response in transport rates as it was observed in time series (Figure 4.5). There was a clear break in slope at about 6.7 mm. R5, in which two pulses entered the system, showed a similar behavior to R1 and R3, but with less variability in transport rates that never reached values as high as in the beginning of R1 or R3. One hour after each pulse (hour 1 and 21), transport rates were relatively high. Ten hours after each pulse (hours 10 and 30) the rates had decreased by about one order of magnitude. Twenty

hours after each pulse (hours 20 and 40), transport rates had decreased again, but not as much as they did during the previous period. An inflection in the trend was observed at ~6.7 mm in most cases, except hour 20. R7 showed a very similar trend to R1 and R3, but the decrease in transport rates was moderate and gradual. There was also a break in slope at about the same size, but at hour 1 it was less clear and could have occurred at a larger grain size.

## 4.4 Sediment storage

To examine the capacity of the system to transfer and store sediment during each run, net change between sediment input and sediment output was computed (Table 4.3). Total sediment input was either zero in runs with no feed, or 300 kg in runs with feed. Total sediment output was estimated from light table data and was different at each run. The ratio between sediment input and output is also presented to give an idea of the overall storage capacity of the system at each run. If there is no feed, this ratio is zero. If it is larger than one, the system is able to store sediment. A larger ratio implies more storage, and as the total input of sediment is constant, it also implies a smaller sediment output.

| Run | Feed regime | Net change (kg) | Input/output ratio |
|---|---|---|---|
| 1 | No feed | -157.88 | - |
| 2 | Constant feed | 218.94 | 3.7 |
| 3 | Episodic feed: one large pulse | 77.48 | 1.3 |
| 4 | Episodic feed: four small pulses | 160.04 | 2.1 |
| 5 | Episodic feed: two medium size pulses | 131.80 | 1.8 |
| 6 | Constant feed | 122.07 | 1.7 |
| 7 | No feed | -58.94 | - |

**Table 4.3. Net change over each run and ratio between total sediment input and total sediment output.**

As the sediment stored during a run was a source for transport for later runs, cumulative storage was estimated and plotted in Figure 4.16, together with net change at each run. However, it is important to consider that the feed material had the same grain size distribution of the bed, and one could expect a larger proportion of coarse material stored because of its partial mobility (as shown in Figure 4.15).

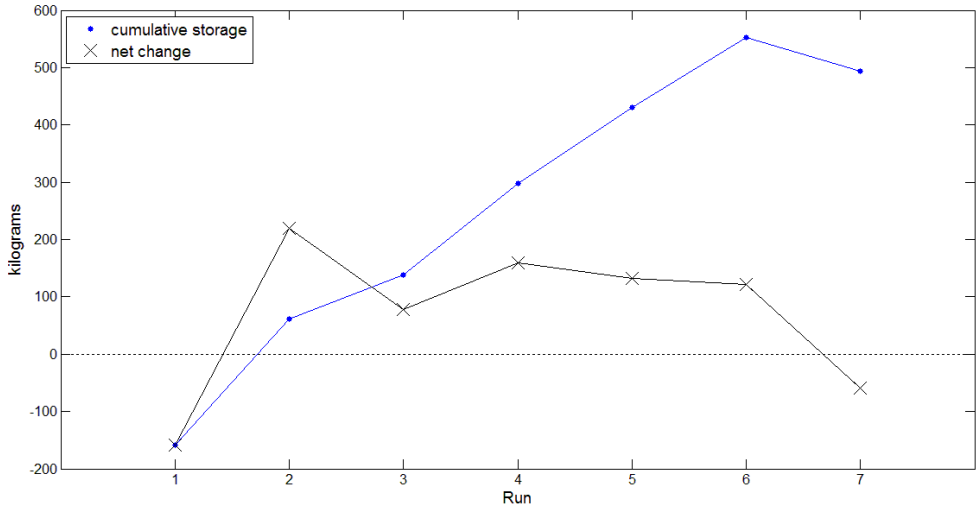


**Figure 4.16. Cumulative storage and net change (difference between input and output) at each run. The dashed line represents zero.**

Cumulative storage showed a general increase through the experiment, with an overall net change of 490 kg. As expected, R1 resulted in net degradation of 158 kg. The large amount of sediment that exited the flume during this run was due to the initial well mixed bed, which had a higher proportion of fines than the armored bed that developed during this run and persisted over the experiment (as suggested by grain size statistical patterns in Figure 4.10). Time series for this run showed that most of the sediment came out during the first hours (Figure 4.1). For R7, which also had no feed, results were different and could be considered more realistic because this run started from a conditioned bed. Sediment output was less than one third of that in R1 (59 kg).

Runs with feed resulted in net storage and overall aggradation. The two runs with constant feed showed different results. This suggests that initial bed conditions played a major role in sediment transport and storage. R2 was the run that stored more sediment (219 kg), with an input/output ratio of 3.7. For R6 instead, the ratio was of 1.7, showing that sediment storage was less significant than in R2 (roughly ½) and more sediment left the flume.

Run 3, in which sediment entered in just one large pulse, had an input/output ratio of 1.3. This indicates that storage was smaller than in all other feed runs and sediment output was more significant (it approached the sediment input). Sediment transport time series (Figure 4.4) revealed that a large amount of material came out during the first ten hours. With four pulses of sediment (R4), the input/output ratio was 2.1, suggesting that sediment input was twice the

sediment output, which was roughly the same amount as stored material (140 kg and 160 kg respectively). In R5, when two pulses entered the system, the input/output ratio was 1.8. Sediment storage was slightly smaller than in R4, and very similar to R6. In spite of these differences in the yield among runs, it was shown that there were little changes in the mobility of sediment and in the particle size of the bed material. It is interesting then to analyze the response of bed slope and channel morphology.

# Chapter 6: Bed evolution

Bed elevations were obtained by scanning the bed several times during each run (see Chapter 3: Methods for more details). These data were used to estimate bed slopes, analyze the temporal and spatial patterns of changes in bed elevation, describe bed topography at the end of each run, and delineate bedforms.

## 5.1 Bed slope

Changes in the slope of the bed were analyzed to identify general trends of aggradation and degradation over the flume during the seven runs. Elevation data was measured relative to the floor of the flume, so it had to be corrected before estimations were done, to add the slope of the flume. A straight line along the flume is not appropriate for bed slope calculations because of the presence of bars and elevated areas. To provide consistent results, a best fit slope was estimated from the thalweg or minimum elevations, as it is done in the field. Minimum elevations were computed at cross sections every 2 mm, which was the resolution obtained from scans. Bed slopes were estimated between 4 and 11.8 m from downstream.

There are no measurements of initial bed slope, but as the bed was flat, it could be assumed that the initial slope was close to 0.0218 m/m (flume slope). The slope showed a slight decrease during the first hour of experiment, reaching 0.0181 m/m (Figure 5.1). During the rest of R1, there were small changes that suggest a very slow decrease towards the end of the run. In R2 there is an increase in slope during the first 20 hours, but at the end of the run (hour 80), the slope was lower than when the feed was started at hour 40.

In R3 there was an increase in bed slope during the first 20 hours, but it was more pronounced than in R2. At hour 120 (end of the run), the slope had decreased, but it was still considerably steeper than the initial slope at that run. The largest variations in bed slope were observed for R4, the run with four small pulses. Slope increased one hour after a pulse, and could remain constant (as with the second and third pulses) or have decreased ten hours after the pulse (as with the first pulse). An increase in slope was noticed overall the run. In R5, there was a pronounced increase in slope one hour after the first pulse. After that, slope continued to increase gradually. After the second pulse there was little change in slope, and this nearly constant trend persisted during R6 and R7. At the end of the experiment, bed slope approached 0.023. This value is very close to the flume slope and well above the slope after the first hour of the experiment. These results are

consistent with net changes obtained in Chapter 5: Sediment transport that showed there was significant net aggradation over the runs that received sediment supply.

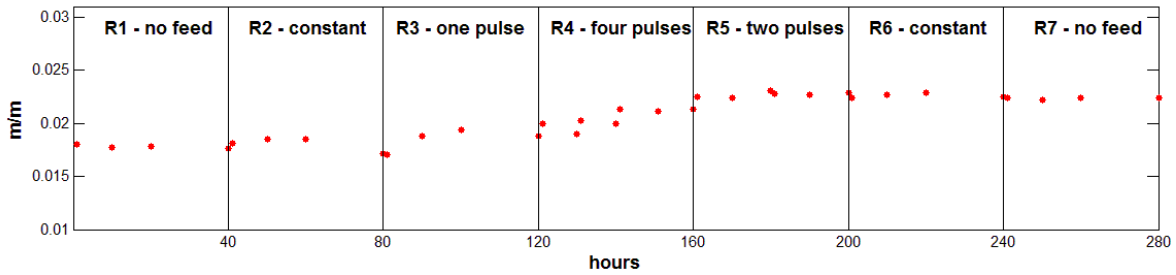


**Figure 5.1. The evolution of bed slope in the thalweg.**

## 5.2 Patterns of aggradation and degradation

Patterns of aggradation and degradation were analyzed by estimating changes in elevation for different periods by subtracting Digital Elevation Models (DEMs). Total aggradation, total degradation and the mean change in bed elevation for periods between two consecutive bed scans were computed to analyze temporal patterns over a relatively large area of the bed (2-11.8 m from downstream). The periods had different lengths depending on scan frequency (one, nine, ten or twenty hours). The net differences estimated over this area do not represent the entire bed and do not match exactly with net changes estimated from the difference between total input and total output. The area upstream of 11.8 m could act as a source of sediment inputs for the analyzed area, so aggradation could be detected during periods of no feed. Mean changes in bed elevation were computed to have an idea of net changes over the studied area. Total aggradation and total degradation provided information about sediment mobilization and re-accommodation.

Degradation was larger than aggradation in all periods of R1 (Figure 5.2). There was a negative mean change in bed elevation, and it was more intense between hours 1-10. Between hours 20-40, the mean change in bed elevation was close to zero (~-0.8 mm). During R2, aggradation was greater than degradation for all periods.

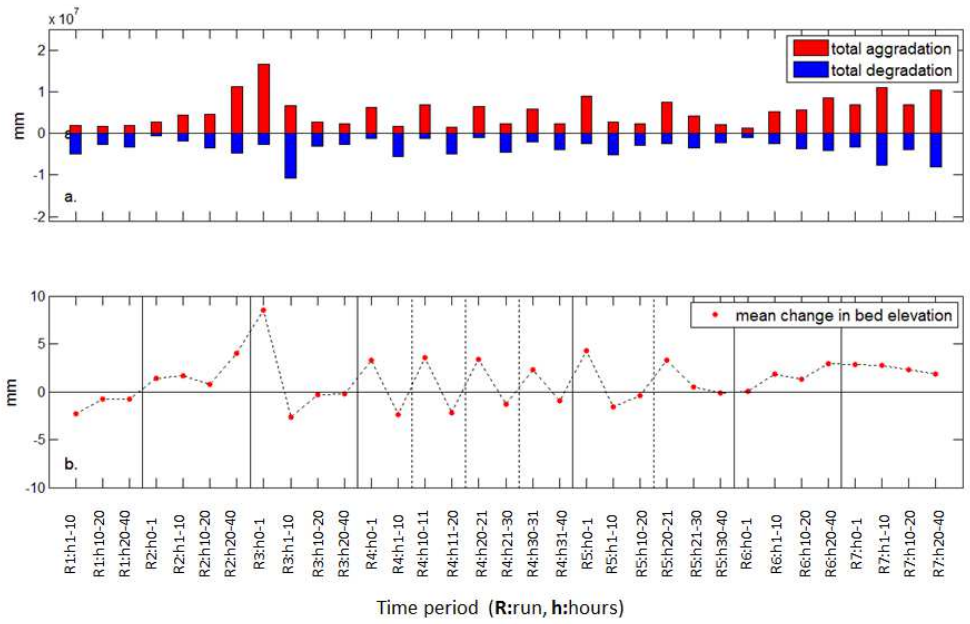


**Figure 5.2. Total aggradation and degradation (a), and mean change in elevation (b) at different periods over the experiment. Estimations were done in the area between 2 and 11.8 from downstream.**

During the large sediment pulse (R3h.0-1), aggradation was significant (6.4 times more than degradation), and mean change in elevation was 8 mm. The following period (hours 1-10) exhibited net degradation (negative mean change). Between hours 10-20 and hours 20-40, aggradation and degradation were small, suggesting low intensity in sediment transport. The mean change in elevation approached zero.

In Run 4, the same behavior was observed after each small pulse. One hour after a pulse started, aggradation was predominant. For the period between one and ten hours after each pulse, there was net degradation. During R5, there was considerable aggradation one hour after each pulse. From hour one to ten after each pulse, aggradation dropped and degradation increased. Finally, 10-20 hours after each pulse, aggradation and degradation were very similar, and the mean change approached zero. In R6, between hours 0-1, changes were also insignificant. After that, aggradation was larger than degradation for all periods. In R7 when the feed was stopped, results showed net aggradation during all periods. This is because the sediment stored upstream in the excluded area acted as a sediment source for the studied area. Even though the mean change in bed elevation was always positive, it showed a decrease and approached zero towards the end of the run.

Overall changes in bed elevations at each run were examined to compare them to the results obtained of net changes between total sediment input and total sediment output. Because initial elevations were missing, in R1 the differences were computed between hours 1-40. In all the runs that had feed, total aggradation was three to four times larger than total degradation (Figure 5.3a) and the mean change exceeded 5 mm (Figure 5.3b). In runs with no feed, there was more degradation, but in R1 the ratio between aggradation and degradation was considerably larger than in R7. In this last run, aggradation and degradation had similar absolute values and mean change was close to zero.

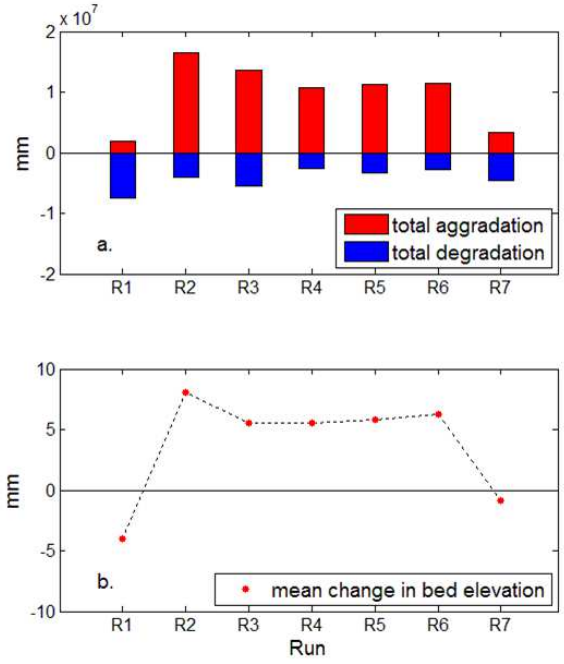


**Figure 5.3. Total aggradation and degradation (a), and mean change in elevation (b) between the beginning and the end of each run.**

Maps showing the spatial pattern of changes in bed elevation are displayed in Figure 5.4. To examine the pattern over each run, changes in elevation were estimated by subtracting elevations at hour 40 (final elevations) from elevations at hour zero (initial elevation). To simplify the observations, changes in elevation were grouped in seven classes: <-30 mm, -10 - -30 mm, -10 - -1 mm, -1 -1 mm, 1-10 mm, 10-30 mm, >30 mm. The resolution of the scan data in the vertical direction is 1 mm. For this reason, values between -1-1 mm were considered as no change.

After R1, most of the bed degraded (Figure 5.4a), and degradation was more intense towards the center of the flume. Aggraded areas were small and well spread. Changes after R2 were more

significant than after R1, especially upstream (Figure 5.4b). Aggraded areas were well differentiated from those that predominantly degraded, and tended to occur at opposite sides. For example, upstream between ~8.5-11.8m, considerable aggradation occurred towards the left side of the flume, where a large area aggraded in more than 30 mm. On the other hand, mainly degradation was observed near the right side of the flume. Between 7-8.5 m, aggradation predominated across the entire channel with moderate (10 - 30 mm) to high values (>30 mm). Downstream between 3-7 m, aggradation occurred towards the right side, but it was less intense than upstream.

In R3 aggradation occurred over similar areas of the bed to R2, but there were important changes upstream of 10 m (Figure 5.4.c). In this area, there was intensive degradation towards the center of the flume (<-30 mm), while both sides mostly aggraded. Downstream, between 2-7 m, aggradation was more extensive than in the previous run.

After Run 4, the pattern was different (Figure 5.4.d). Upstream of 8 m there was degradation towards the center (a little bit shifted to left), and aggradation towards the sides, being especially important on the right side (>30 mm). Downstream of ~8 m the pattern was complex, with intercalation of aggraded and degraded areas with transverse orientations. In R5, it is possible to see what happened upstream (up to 13 m). Over this area the bed probably aggraded because of the sediment supply (Figure 5.4.e). From 7 to 11.5 m, significant aggradation occurred towards the right, whereas the left side mostly degraded (except for a narrow area just beside the flume wall). Downstream, the pattern remained complex, but not exactly the same as in R4.

After R6, the spatial pattern of changes in elevations is complex (Figure 5.4.f). General lateral differentiation between aggraded and degraded areas is appreciated, but it is overlapped with the intercalation of smaller aggraded and degraded areas. Downstream degradation extends over a larger area than after R5. Results for R7 are presented in Figure 5.4.g, and show that changes in elevation are less pronounced. Most of the bed went under moderate aggradation or degradation (-10-10 mm). There were some specific areas that aggraded more intensively, usually closer to areas that degraded more intensively.

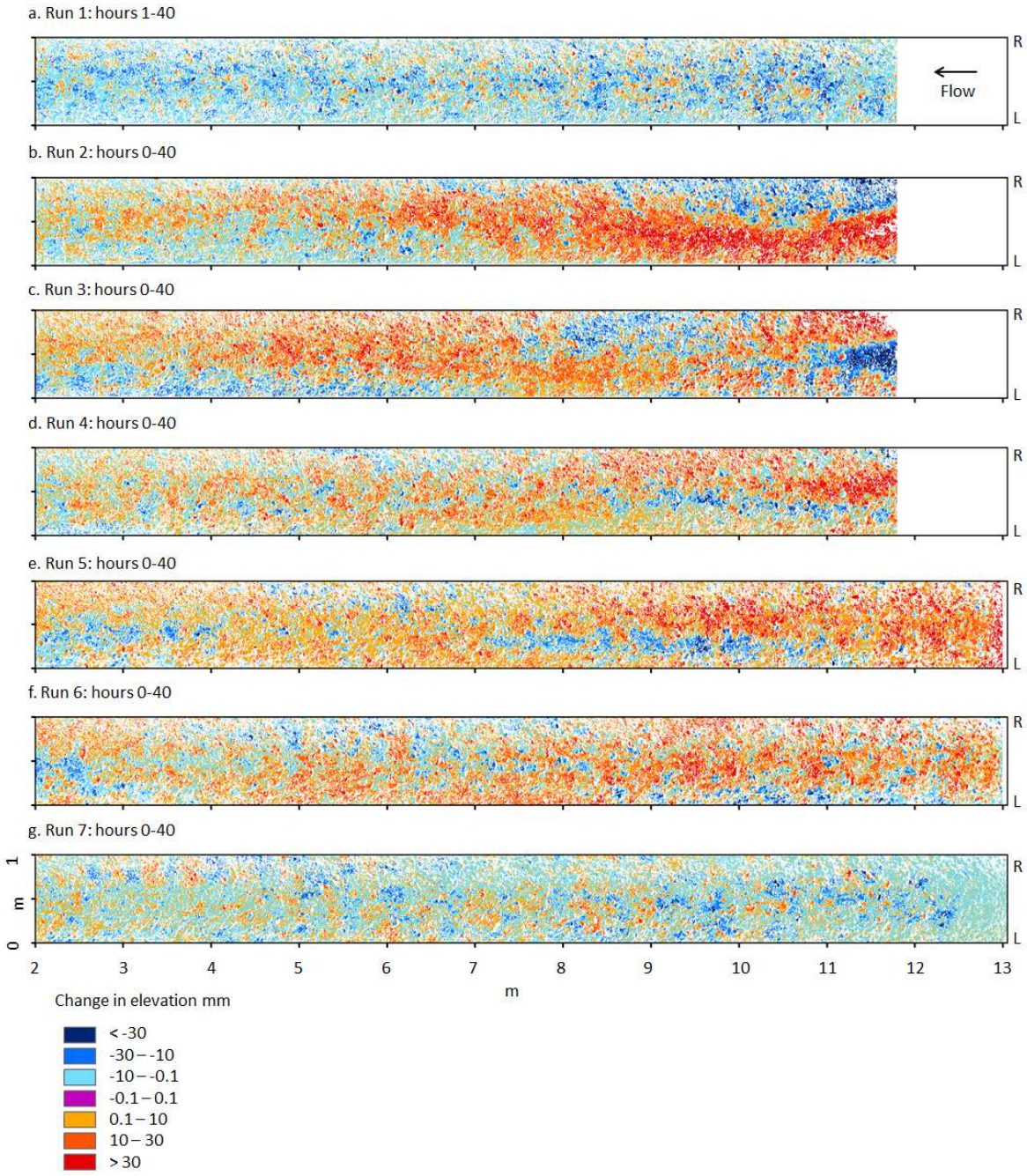


**Figure 5.4. Spatial pattern of changes in elevation, between the beginning and the end of each run. R: right, L: left. Distance in the longitudinal direction is given relative to the downstream end of the flume.**

## 5.3 Bed topography

In the literature, the presence of bedforms has been linked to sediment supply and transport regimes, and attributed important functions in flow resistance and sediment storage. At smaller scales, bed structures such as clusters, ribs and stone cells might increase flow resistance and energy dissipation, and reduce sediment mobility. At larger scales, bedforms like riffle-pool sequences and bars are very important for flow resistance and sediment storage. To identify and describe the presence of bedforms in the flume, bed elevations were used. The spatial resolution of the data (2 mm) allowed the analysis of bed structures, but the evolution of microtopography was not analyzed (see von Flotow, 2013 for results regarding microtopography). The classification provided by Hassan et al. (2008) was used as a guide and the focus was on macroforms and mesoforms like bars and riffle- pool sequences.

To reduce the variations caused by the presence of particles of different sizes and better identify trends due to bed morphology at a larger scale, the DEMs were smoothed in the transverse direction. A running mean with a window length of roughly the maximum particle size in the bed (70 mm=35 points) was applied. Smoothed elevations were displayed in different ways (stretched, and classified with different ranges from 10 mm to 20 mm). Classified data was better at identifying changes between runs, and a range of 15 mm was enough to observe small differences due to bedforms. All elevations below 50 mm were considered low and grouped in one class. All elevations higher than 140 mm were rare, so they were grouped. Minimum elevations were displayed with a specific color for an easier identification of the thalweg.

In the field, large scale bedforms such as bars are defined relative to the flow (exposed area at a given flow, usually base flow). However, no objective method for the delineation of bars is available. As an alternative, bedforms were defined from the DEMs, using slope inflections in the transverse direction to delineate the boundaries. Cross sections of raw and smoothed elevations were plotted every 100 mm to identify major inflection points that could be used to delineate the bedforms. Inflection points were displayed on top of the DEMs and bedforms were delineated, also taking into consideration the trends at a larger scale than the cross section. Even though the method was done in a systematic way, there was subjectivity delineating the bedforms. Some cross sections are plotted as examples in Figure 5.5.

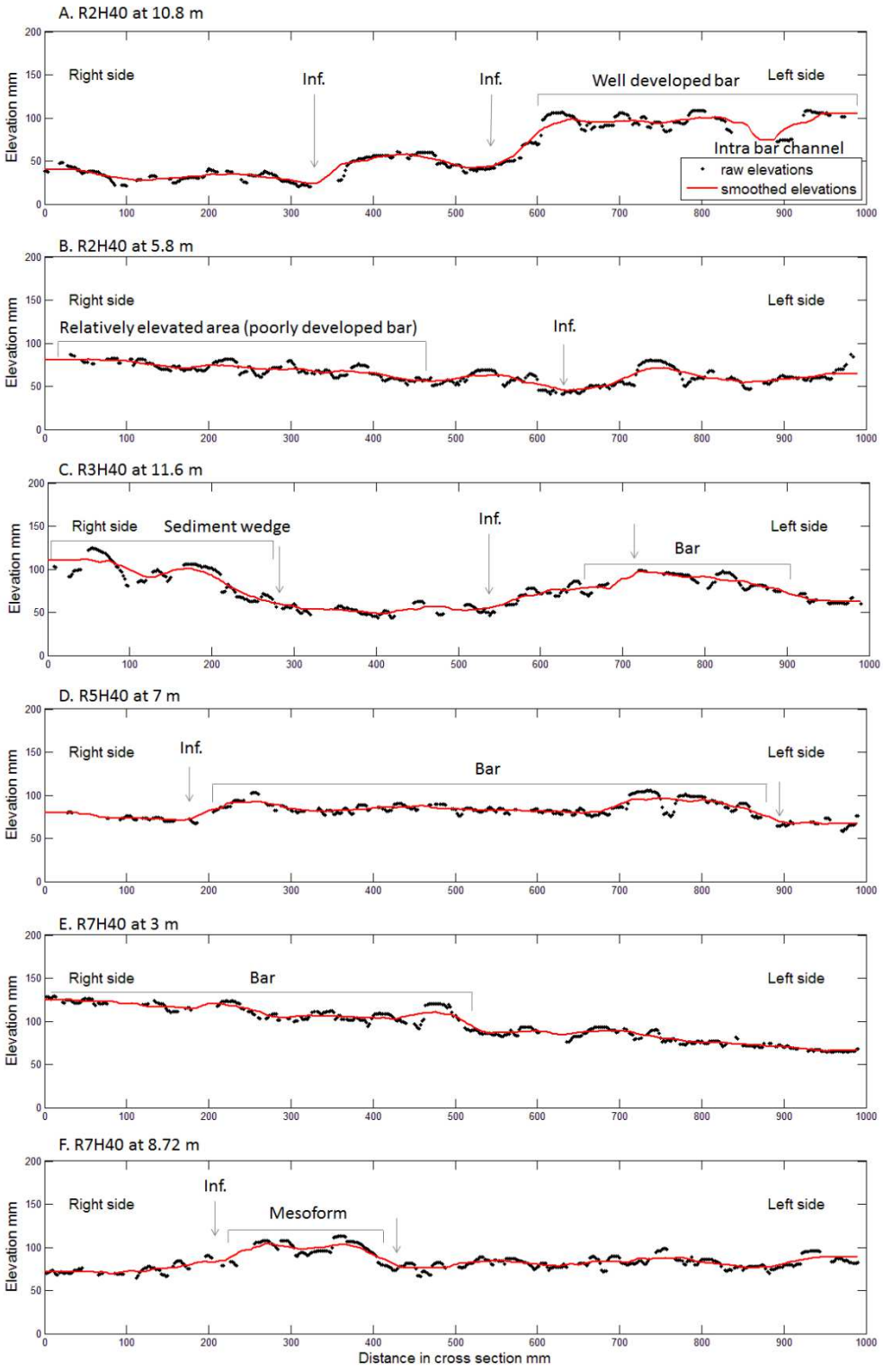


**Figure 5.5. Cross sections of bed elevations used for bedforms identification. The black line corresponds to raw data and the red line to smoothed elevations. Arrows point out inflection (Inf).**

There were cross sections that exhibited a well differentiated topography with clear inflections, suggesting the presence of well-developed bedforms, as the one in Figure 5.5.a. In this cross section there is a base level (low flow channel level), and towards the left side, there are two inflections that mark relatively elevated areas. There is a small step with elevation only a few cms above the base level, and a large step or upper level where elevations are significantly higher (~7 cms above the base). In some cases, cross sections exhibited just one infection in its lowest point and an increasing trend towards one of the sides (Figure 5.5.b.), or just an increasing trend with no inflection (Figure 5.5.e). If the differences in elevation were significant and the same trend was observed over a few meters, a bar or wedge was delineated over the side where elevations increased. In another cases, inflections defined elevated areas towards the center of the flume. If this trend was repeated in cross sections along a few meters, a bar in the middle of the channel was delineated as in Figure 5.5.d. If the trends were local (only occurred in few sections), mesoforms such as riffle-pools were noticed, but not necessarily delineated in the maps (Figure 5.5.f).

Maps with elevations and bedforms at the end of each run are presented in Figure 5.6. Distances in the longitudinal direction are relative to the downstream end of the flume. At the end of R1 (after 40 hours of no feed), the thalweg plotted towards the center of the flume upstream, and was surrounded by a large area that had very low elevations (<50 mm). Downstream, between 2 and 4 m the bed was relatively elevated and the thalweg suggested more than one low flow path.

Different patterns of bed elevations and channel morphology were obtained at the end of R2 (Figure 5.6b). The thalweg was situated in the right side upstream and shifted towards the left side downstream. Important transverse differentiation of bed elevations were observed in the map due to the presence of bedforms. Upstream of 8 m, a sediment bar appeared in the left side of the flume. It was relatively high and well defined as seen in Figure 5.5.a. A second bar developed downstream on the opposite side between 2 and 5 m. The differences in elevation between this bar and the rest of the channel were not as significant as for the upstream bar, and the bedform was poorly developed (possibly under formation). The pattern of elevations over the central area of the flume (6-8 m) was complex, suggesting a transition zone with alternation of elevated and depressed areas that could be related to mesoforms.

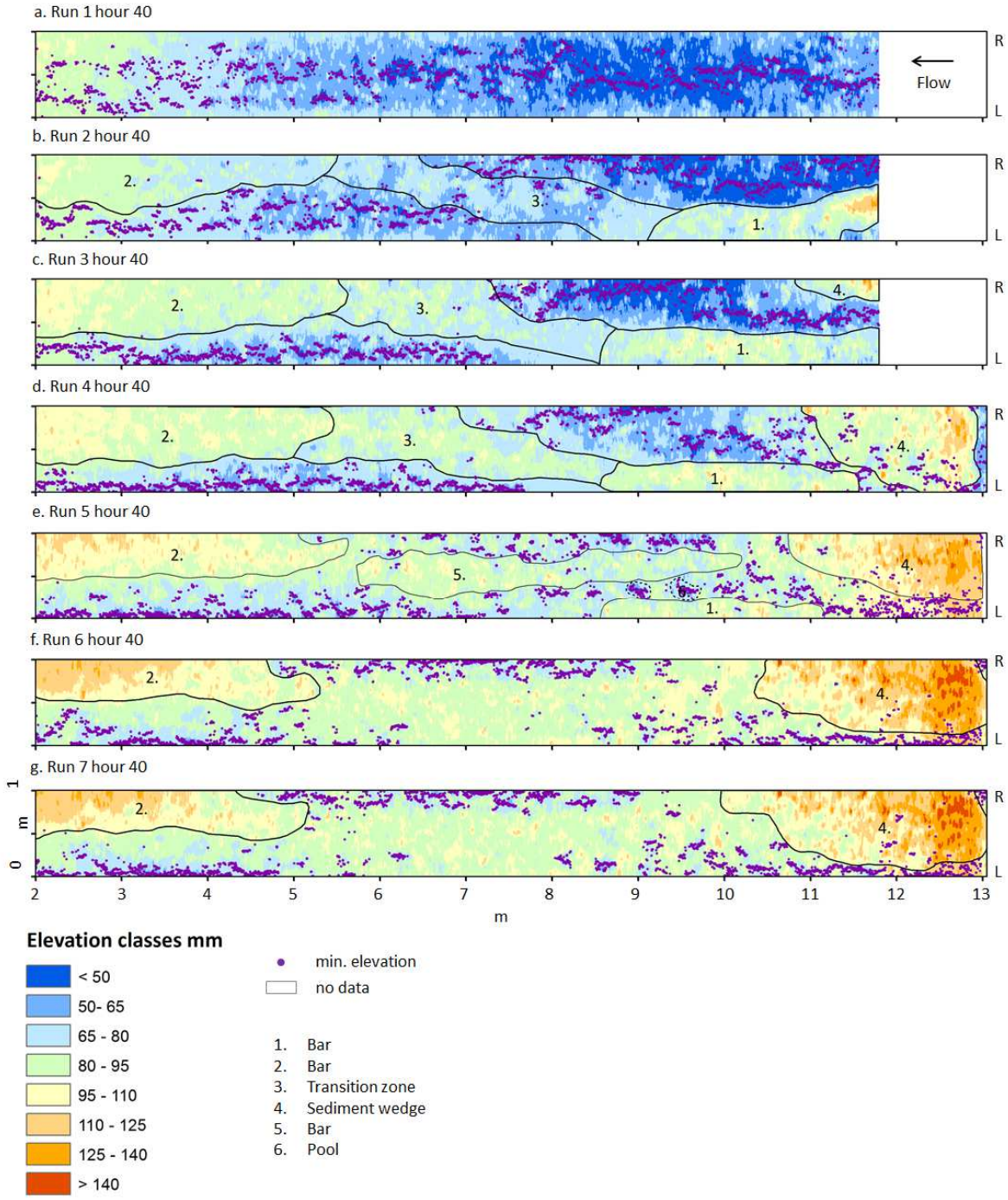


**Figure 5.6. Spatial patterns of bed elevation at the end of each run.**

After R3, spatial patterns of bed elevation were similar to those of R2 (Figure 5.6c). The thalweg showed the same path as in R2, except upstream of 10 m. Here, it shifted towards the center of the flume because of the appearance of a new elevated area in the right side. This area was defined as a sediment wedge because subsequent observations gave information of what was

happening further upstream. The bar on the left side upstream lengthened in the downstream direction. The elevation of the bar downstream increased significantly relative to the end of the previous run. The same occurred in the transition zone.

At the end of R4, the configuration of bed elevations was similar to the end of R3 (Figure 5.6d). Data from upstream revealed the presence of a large sediment wedge that projected downstream until ~11 m. In this area, the thalweg moved towards the left side. The upstream bar on the left side didn't exhibit important changes, while the transition zone and the bar downstream clearly aggraded. At the end of R5, the spatial pattern of bed elevation was significantly different from previous runs as seen in Figure 5.6.e. The thalweg suggested a bifurcation of low flow paths between ~6-10 m because of the appearance of a bar in the middle of the channel, as it was shown in Figure 5.5.d. It also suggested the presence of pools. The sediment wedge extended downstream. The upstream bar in the left side was significantly smaller than before, whereas the downstream bar persisted and aggraded.

Results at the end of R6 reveal interesting changes in bed morphology and are presented in Figure 5.6.f. Upstream, the thalweg was located in the left side. At about 10 m it shifted to the right, and at 5 m, it shifted to the left again. The wedge of sediment upstream aggraded significantly. Aggradation was also important between 5-10 m, transforming the mid channel bar in a very large elevated area that extended almost across the entire channel. Here, low elevations were confined to a narrow zone towards the right or gathered over small areas, suggesting the presence of depressions or pools. The upstream bar at the left side of the flume disappeared and morphology of more like riffle-pool sequences was built. The downstream lateral bar persisted and aggraded. Little changes in elevation were observed after R7, and spatial patterns of bed elevation at the end of the run were very similar to those at the end of R6 (Figure 5.6g).

# Chapter 7: Discussion

The main objective of this study was to examine the impact of episodic sediment supply regimes on sediment mobility, bed evolution and channel morphology. High spatial and temporal variability was expected during the experiment due to changing sediment supply. Runs with no feed were expected to behave as low supply regimes (Parker & Klingeman, 1982; Dietrich et al., 1989; Church et al., 1998; Hassan & Church, 2000; Ryan, 2001; Church & Hassan, 2002; Hassan & Woodsmith, 2004), and it was expected that each time the feed was stopped there would be a decrease in transport rates due to bed surface structuring, and/or a decrease in slope due to degradation. Each time sediment entered the system, it was expected to produce aggradation, fining of the bed surface and an increase in transport rates. A rare large sediment pulse could produce a significant increase in the intensity of sediment transport over a relatively short period of time (passage of a sediment wave) that could change significantly the bed surface composition (surface fining and destroy bed structures), increasing transport rates in the outlet of the flume. After some time, the system could behave as under no feed (coarsening and/or slope decrease, reduction of transport rates). If the pulses were smaller and entered more frequently, the system could behave similar to constant feed regimes.

The discussion is divided in two sections. The first one attempts to answer how important the way in which the sediment entered the system was for the adjusting sediment mobility, GSD of the bedload and the bed surface, bed slope, net changes in bed elevations and the bed macro topography. The idea is to compare constant feed and episodic regimes, as well as comment on the importance of pulse size and frequency in the episodic regimes. As the initial bed was different for each run, it is interesting to explore the importance of the initial conditions (bed history) in the results. For this reason, in the second section the adjustments of the variables discussed in the first section are commented in detail for runs with the same feed conditions.

## 6.1 Channel adjustment under different supply regimes

Changes in sediment supply produced adjustments in the channel, which were conditioned by the way in which the sediment entered the system. A summary of adjustments under each run is presented in Table 6.1.

| Run | Feed regime | Channel adjustments to changes in sediment supply | | | | | | |
|---|---|---|---|---|---|---|---|---|
| | | Sediment mobility | | Particle size | | Bed elevations | | |
| | | Transport rates | Relative mobility | Bedload | Bed surface | Bed slope | Net changes | Bedforms at the end |
| **1** | No feed | General decrease, very pronounced during the first hours and then gradual. | No significant changes. | Slight fining. | Coarsening | Small changes | Net degradation | Central channel, lack of bedforms. |
| **2** | Constant feed | Relatively slow response. Small and gradual increase and high variability. | No significant changes. | Oscillating | Oscillating | Increase during 20 hours and then decreased. | Net aggradation | Alternated lateral bars and a transition zone in between. |
| **3** | One pulse | Significant increase in less than one hour since the feed followed by monotonic decrease with sporadic spikes. | No significant changes. | Fining (no coarsening after the pulse). Similar to R7. | Significant fining after the pulse followed by coarsening | Increase followed by slow decrease. | Aggradation after the pulse followed by degradation . Little changes towards the end of the run. | Similar bedforms as in R2, but more elevated. |
| **4** | Four pulses | Increase after each pulse. The response was smaller than in R3. Similarities with constant feed (i.e. in the variability) | No significant changes. | Coarsening after each pulse followed by fining. | Same response as R3 after each pulse, but fining was less significant. | Increase one hour after each pulse. Ten hours after the first pulse the slope decreased, but with the others it remained high after ten hours. | Aggradation after each pulse followed by degradation . | Similar to R3, Sediment wedge upstream because of the feed has expanded. |
| **5** | Two pulses | Similar response to R3 after each pulse. | No significant changes. | Similar to R4 | Similar to R4 | Increase after the first pulse. Nearly constant values after the second pulse. | Same pattern as R3 after each pulse. | Lateral bars and mid-channel bar, riffle pool sequences. |
| **6** | Constant feed | Same trend as R2, but higher values. | No significant changes. | Oscillating, small coarsening ~7 hours after the feed started. | Fining and then coarsening | Nearly constant. | Net aggradation | Riffle pool sequences upstream. Persistence of the lateral bar downstream. |
| **7** | No feed | Small decrease | No significant changes | Gradual fining | Coarsening | Nearly constant | Net degradation | Almost the same as R6 |

**Table 6.1 Summary of channel adjustments under seven runs with different sediment supply regime.**

As expected, total transport rates were significantly affected by the changes in sediment supply. Each time the feed was started, transport rates increased, and then decreased after the feed was stopped. The way in which transport rates changed was different for each run, and it was strongly related to the way in which supply entered the system. Under constant feed (R2, R6), transport rates showed a moderate increase at the outlet of the flume seven or eight hours after the feed was started. Under episodic supply (R3, R4, R5), the increase in transport rates occurred faster (less than one hour) and it was followed by a decrease until transport rates were similar to those before the pulse or a new episode entered the system. The fast response could be due to piling of sediment upstream with each pulse and an increase in slope, but also to a larger amount of fine material available to be easily transported. Fractional transport rates showed that smaller grains (<8 mm) moved with higher intensities and were more affected by the changes in supply than coarser fractions. During periods of no feed (i.e. between pulses), the availability of smaller fractions on the bed surface was reduced because of winnowing, infiltration or structuring.

The size of the pulse was important for the response of transport rates. The 300 kg pulse produced the largest increase in transport rates and it even showed a secondary response at about the same time as the response under constant feed (seven hours). This could be due to sediment that moved more slowly through the system. After fifteen hours, transport rates were low as in no feed regimes and towards the end of the run. The response in sediment transport rates to the 150 kg pulses was similar to the response to the 300 kg pulse. The increase in transport rates produced by each 75 kg pulse was considerably smaller, especially after the third pulse. The frequency of sediment inputs was important and the run with the four pulses showed some similarities to constant feed regimes as in the short term variation. In general, five to ten hours after each pulse (no matter the pulse magnitude), transport rates presented similar values to those before the pulse. This doesn't mean that the channel recovered from the effects of the pulse. As it will be discussed later, cumulative storage, bed slope and bed morphology showed that the effects of sediment supply persisted over the bed and were cumulative during the experiment.

The bed surface and the bedload textures showed opposite trends to changes in supply as expected. The textural adjustment of the bed surface was conditioned by the initial bed, flow competence and supply regime. When there was feed, the regular transport of fine material could produce fining of the surface. It has been suggested that a higher proportion of fines on the surface affects entrainment conditions, promoting the transport of coarser material (Wilcock &

Crowe, 2003; Venditti et al., 2010). In our experiment, the coarsest values of the $D_g$ and $D_{16}$ of the bedload were obtained when the bed surface was relatively fine. After the feed was stopped, fine material winnowed or infiltrated, and transport rates declined as the bed surface got coarser and the bedload got finer.

Particle size adjustments of the bed surface and bedload were different under episodic and constant feed regimes. Under constant feed, the bed surface's texture showed a complex temporal pattern and fining was not always evident. For example, in R2 the $D_g$ and $D_{16}$ of the surface were fluctuating and small coarsening was observed towards the end of the run. In R6, the surface got finer during the first fifteen hours, but then it coarsened and remained almost constant towards the end of the run. The bedload textures under constant feed exhibited variation and small coarsening. It has been mentioned that in sediment feed flumes the GSD of the bedload should approach the GSD of the feed when equilibrium is achieved (Parker & Wilcock, 1993), but in our constant feed runs the bedload GSD was always finer than the GSD of the feed. This suggests no equilibrium was reached during these runs and that a longer period of constant feed might be necessary to coarsen the GSD of the bedload until it approaches the GSD of the feed.

Under episodic regimes, bed surface texture showed a clear inflection related to each pulse. One hour after each pulse, the surface got finer and then it coarsened as fines winnowed and infiltrated under no feed conditions. The texture of the bedload was coarse right after each pulse and it got finer as the surface coarsened under no feed conditions. The size of a pulse was important for the rate of change on the bed surface. For example, the fining was more pronounced with the largest pulse, and the following coarsening was faster. The rate of change in bedload texture was less dependent on the size of the pulse. For example, with the largest pulse the texture remained unchanged, while with the first of the smallest pulses the response was significant. These reflected the importance of initial conditions.

As explained before, sediment pulses increased the proportion of fine material on the surface over a short period of time. As the proportion of fines on the bed surface is important for gravel entrainment (Curran & Wilcock, 2005; Venditti et al., 2010), one could expect the intensity of transport of coarser fractions to increase. Our experiment showed that regardless of small changes in fractional transport rates, the movement of coarser fractions was always of low intensity and sporadic. Most of the time, the limit between partial transport and fully mobilized

transport occurred at 6.7 mm. The occasional movement of grains and fluctuations in transport rates produced small changes that could not be explained by changes in transport rates due to supply regimes. For example, during R3 fractional transport rates spanned over two orders of magnitude due to changes caused by the large pulse, but the limit of partial mobility remained constant. This suggested that the effects caused by fining and smoothing of the bed surface by the pulses were not strong enough to change the relative mobility of coarse fractions.

To explore the system´s overall storage capacity during each run, net changes in the bed were presented in two ways: net storage estimated as the difference between sediment input and sediment output (Figure 4.16); and net changes in bed elevations over a large area of the bed (Figure 5.3). As the area considered in each method was not exactly the same, there were some differences in the results, but the trends were consistent. As expected, runs with no sediment supply resulted in net degradation. All runs with sediment feed showed net aggradation, and the cumulative storage over the entire experiment was close to 500 kg. The large amount of stored sediment could be due to the relatively coarse and poorly sorted texture of the feed material. Fractional transport rates during the experiment showed that coarser fractions moved with low intensity. The results of relative mobility analysis suggested grains larger than ~8 mm were partially mobile and the texture of the bedload was finer than the feed texture. All these suggest that a large proportion of the coarse fractions that were supplied remained in the bed.

The way in which the sediment entered the system influenced the storage capacity. As the 300 kg pulse generated a large output of sediment, the sediment stored over this run was considerably less than with constant feed regimes when the sediment entered slowly and the bed had more time to adjust. Runs with smaller and more frequent pulses showed more storage, similar to constant feed regimes. The interesting difference noticed between the two runs with constant feed suggested that the initial conditions were important for storage capacity. Cumulative storage revealed that the effects of sediment supply in the bed were persistent.

The thalweg slope was sensitive to changes in sediment supply, but there were also cases in which it remained constant after feed input (e.g. after the second 150 kg pulse in R5 or during R6). During runs with no feed, there were little changes in slope and during runs with feed a general increase was noticed, probably due to net aggradation in the bed throughout the experiment. Runs with constant feed showed different adjustments (in R2 there was a small increase in slope during the first 20 hours and then it decreased, while in R6 it was almost constant during the

entire run), but in both cases, the final slope was close to the initial slope. Under episodic supply, there were larger increases in slope after each pulse than under constant feed (except after the second 150 kg pulse in R5, in which the slope remained constant) and the final slope at each run was steeper than the initial slope. After the 300 kg pulse, the increase in slope was slower than after 75 kg pulses (one hour after the large pulse the slope had not changed). After sediment pulses the bed slope never went back to the values previous to the pulse. The only exception was after the first of the 75 kg pulses. These results showed that the effects of episodic sediment supply in the bed slope could be persistent and no recovery was observed after starvation periods. This brings up the question of how long would it have taken the bed to get the same slope as before a sediment episode, or if it is likely to happen.

Mean changes in bed elevations were influenced by the area of the bed covered by the scans that didn't include the upstream end; but in general, net degradation under no feed conditions and net aggradation over periods with feed was observed. As expected, runs under constant feed showed aggradation, and episodic regimes presented short periods of relatively large aggradation determined by feed duration and longer periods of degradation given by the pulse frequency. In all the cases, degradation during no feed periods was less significant than the aggradation during feeding periods and the changes were very small ten or twenty hours after each sediment episode. One hour after the 300 kg pulse, aggradation was larger than after smaller pulses, but it was commented before that net storage was considerably more over the runs with more frequent and smaller pulses.

The initial bed and flow configuration strongly influenced the spatial distribution of changes in elevation. Aggraded and degraded areas of the bed presented well differentiated patterns consistent with the development of bedforms. During R2 and R3, aggradation occurred mostly towards one side of the flume and shifted in the downstream direction. This was probably related to the formation and accretion of lateral bars. Towards the opposite side of the flume, degradation predominated. After R4 (four pulses), the pattern changed. The intercalation of aggraded and degraded areas with transverse orientations that could be related to the formation of riffle-pool sequences or other transverse features was observed. During the last run, as there was no sediment feed, changes were relatively low.

The configuration of bed elevations at the end of each run showed that the bed morphology evolved from a featureless state during no feed in R1 to well-developed bars and riffle-pool

sequences that persisted after no feed conditions in R7. As expected, most interesting changes occurred after runs that received sediment feed. The changes implied the appearance of new bedforms (i.e. after R2), the accretion of the existing features (i.e. after R3), or their disappearance and transformation (i.e. after R5). The evolution of the bed topography can be summarized as follows. At the end of R1 the bed lacked features and the thalweg plotted towards the center of the channel. After R2 lateral sediment bars were insinuated in the bed and the thalweg switched to the opposite side of each bar. The formation of bars could be explained by the spatial variability in sediment transport rates (suggested by the spatial patterns of aggradation and degradation), as a result of the way in which the sediment entered the system and affected the distribution of the flow. Even though it did not appear in the scan, a sediment wedge was created upstream due to the feed. The wedge consisted mostly of the coarse material that was difficult to be transported. The wedge expanded downstream during the experiment and became larger each time that supply entered the system. After R3, bed elevations increased and the final bed morphology at R2 conditioned the evolution of the bed during R3. The bars observed after R2 persisted and grew, and the sediment wedge extended downstream. After R4 the bars persisted, but the bar upstream degraded (bar 1 in Figure 5.6). The sediment wedge upstream aggraded.

After R5, the topography exhibited interesting changes. The thalweg changed significantly, insinuating a divergence of low flow paths in the center of the flume and the presence of pools. Also, a mid-channel bar was identified. It is unlikely that the interesting topography after R5 could be explained by the sediment supply regime (two 150 kg pulses). These results were probably conditioned by the initial bed, which was the result of the history of supply episodes and their cumulative effects over the channel. After R6 there was important filling of the bed and only the downstream bar persisted. The sediment wedge expanded, and downstream of it, riffle-pool sequences were insinuated. After R7 (no feed) changes in elevations were very small, and the topography was almost the same as after R6.

Even though it was commented that the way in which the sediment entered the system was important for net changes in elevations (amount of sediment accumulated over a run), the bed morphology could not be explained by the supply regimes. The spatial variability of sediment transport rates and the evolution of topography during a run were conditioned by the initial bed. For this reason, it was observed that runs with the same supply regimes exhibited final bed

morphologies that were significantly different. This idea will be discussed with more detail in the following section.

## 6.2 The importance of the initial conditions

The initial bed at each run was different because of the way in which the experiment was conducted and influenced the results at each run. It was observed that runs with same feed regimes presented differences in transport rates, the amount of sediment stored, ranges of bed slope, and bed morphology. Differences were also noticed after sediment pulses of the same size and were attributed to the conditions of the bed at the moment that the pulse entered the flume. The idea of this section is to discuss the importance of the initial bed in the adjustment of the variables presented above. To do this, the adjustments under the same feed conditions will be compared in detail in an attempt to explain their differences.

Run 2 and Run 6 had a constant feed regime and provide a good opportunity to discuss the importance of the initial bed. The initial bed at R2 was the result of 40 hours of no feed and had a slope of ~0.018 m/m. The surface was relatively coarse ($D_g$ of ~15 mm) and no macroforms due to sediment accumulation were present. The initial bed in R6 was conditioned by the supply history and bed evolution during all the previous runs. It also had a relatively coarse surface ($D_g$ of ~15 mm), but it also exhibited a more complex morphology with bedforms at different scales. The bed slope was ~0.023 m/m, very different from the initial slope in R2 and suggestive of aggradation during previous runs.

The temporal patterns of transport rates in both runs were similar (response to the feed at roughly seven hours, large variability, small increase towards the end of the run), but transport rates didn't exhibit the same values. The values plotted slightly higher during R6, which could be related to the large amount of sediment accumulated during previous runs that generated steeper slopes during this run, and a smaller storage capacity than in R2. R2 stored 219 kg, with a sediment input/output ratio of 3.7. The ratio for R6 was 1.7, showing that sediment storage was roughly half the storage in R2.

The bed surface was relatively coarse in both cases ($D_g$ between ~13-15 mm), but it was slightly finer in R6 and textural adjustments were different at each run. In R2, there was significant fluctuation, and a small coarsening in the $D_g$ was noticed towards the end of the run. In R6 the pattern was different and there was fining during the first fifteen hours. At hour 20 the surface

coarsened and remained nearly constant towards the end of the run. As it was already mentioned, bed slope was steeper during R6. During R2, there was small increase in slope as a response to sediment supply. During R6, bed slope was almost constant, suggesting there were no important adjustments of the slope due to the changes in sediment supply.

In addition to the interesting differences in bed elevations because of cumulative storage during the experiment (the bed was significantly more elevated after R6 than after R2); there were significant differences in the bed morphology. The wedge of sediment that started forming upstream in R2 due to the sediment feed had increased considerably after R6 and expanded in the downstream direction. The well-developed bar that was observed upstream in the right side of the flume after R2 had disappeared after R6, and riffle-pool sequences developed in its place. The bar that was identified downstream on the right side after R2 was still present in R6, but it was significantly more elevated. The thalweg did not exhibit the same path after each run. In R2 it shifted from the right side upstream to the left downstream. In R6 instead it shifted twice: from the left upstream to the right in the middle, and then to the left downstream again.

Significant differences were also observed under no feed conditions (R1 and R7) due to differences in the initial bed. R1 started from a well-mixed leveled bed with high proportions of fine material available for transport and no bed structures. Because of the winnowing of fines, transport rates in the beginning of the run were high and exhibited rapid decrease during the first hours. The initial bed for R7 had a complex morphology with riffle-pool sequences, a bar downstream, and a relatively large sediment wedge upstream. The initial bed surface was coarser (armor ratios: 2-4), exhibited structures, and had a lower proportion of fine material than in R1. For this reason, transport rates were considerably lower during the first hours, showing slow and gradual decrease over the run. Regardless the first hours, R1 exhibited important variability. R7 instead exhibited small variability and slightly higher rates. This could be related to steeper slopes and the large wedge of sediment upstream, due to net aggradation that occurred during the past runs.

Because of differences in the initial conditions, total sediment output in R1 was almost three times more than in R7, which had steeper bed slopes. As expected, the bed topography was also significantly different. In R1, the relatively flat initial bed degraded upstream and at the end of the run it was more elevated downstream. In R7, changes in bed elevations were relatively small and the bed exhibited a complex topography very similar to the topography at the end of R6 with riffle-pool sequences and a bar downstream.

Pulses of the same size provide an opportunity to analyze the importance of the bed conditions under episodic supply regimes. There were interesting differences in the temporal patterns of transport rates after each small pulse. For example, the increase in transport rates at the end of the flume after the third pulse was very small, while after the last pulse it was relatively large. For example, after the first pulse an increasing trend persisted over one or two hours before it started to decline; whereas with the last pulse, there was significant increase in transport rates and immediately after that, the rates started to decrease.

A good example of the importance of the initial conditions was observed in the textural adjustment of the bedload. The degree of coarsening that followed a supply episode could not always be explained by the size of the pulse, showing a strong relation with bedload textures previous to the pulse. This could be controlled by the previous feed conditions. If before the pulse there was feed and the texture of the bedload was relatively coarse, the pulse slightly changed the texture, like in R3. If the pulse came after a long starvation period and the texture of the bedload was relatively fine, the effect of the pulse on the texture was significant. For example, after the first of small pulses in R4 that came after 39 hours of no feed, the texture of the bedload coarsened significantly.

# Chapter 8: Conclusions and future work

The goal of this study was to analyze channel adjustments under episodic supply regimes. This objective was achieved by conducting a flume experiment that combined a sequence of runs with different sediment feed regimes, but constant feed GSD and water discharge. From the observations and analysis the following conclusions can be drawn:

- Changes in sediment supply produced interesting effects in sediment transport rates, the texture of the bedload and the bed surface, sediment storage, bed slope, and bed topography. The way in which the changes occurred was different between constant feed and episodic regimes. Under constant feed, all variables adjusted slowly and gradually. Episodic supply instead could produce pronounced changes just after a pulse, depending on the size of the pulse and the conditions of the bed.
- The results indicate that sediment transport rates are affected by episodic supply. Soon after each pulse, transport rates at the end of the flume increased, and after some time, started to decrease until reaching values similar to those before the pulse. The size of the pulse was important and largest pulses produced considerably larger increases. The frequency was also important because the run with small pulses every ten hours (R4) showed more short term variation as constant feed regimes did.
- The temporal adjustment of the texture of the bed surface and bedload had a similar pattern to transport rates. A pulse produced significant changes; but after some hours, the variation was small and conditions similar to those before the pulse were observed. The bed surface texture got finer just after each pulse, and then it coarsened. The texture of the bedload showed the opposite trend. It was coarser when the surface was finer, and became finer when the surface coarsened. The fining of the bed surface was more significant after larger pulses. The degree of coarsening in the bedload was not related to the size of the pulse, and it depended on the initial bedload texture, which was influenced by the previous feed regime. For this reason, the largest sediment pulse, which came after a run with constant feed, did not have a coarsening effect on the bedload.
- The relative mobility of sediment was not significantly affected by changes in sediment supply and the limit between partial transport and full mobility remained almost constant at 6.7 mm. This suggests that fining and smoothing of the bed surface caused by sediment

pulses was not strong enough to change the relative mobility of coarse fractions and make them fully mobile.

- Sediment storage was significant during all runs with feed, revealing that the effects of sediment supply over the bed were cumulative. The size and frequency of the inputs under episodic regimes was important. The largest pulse caused considerably less storage due to the large response in transport rates. The storage under runs with smaller and more frequent pulses was more similar to constant feed regimes.
- The bed slope did not always adjust to the changes in sediment supply. Under runs with constant feed, the slope was nearly constant or exhibited few changes. Under episodic regimes, in most cases the slope increased after a pulse, and then remained constant or slightly decreased until a new pulse entered the system. The increase in slope could not be explained by the size of the pulse and after the second 150 kg pulse, the slope remained constant. It is concluded that the effects of sediment supply on slope were persistent without recovery of slope under periods of no feed.
- The bed topography evolved during the experiment, showing most changes during runs with sediment feed. Changes in bed elevations were relatively small when there was no feed. The bed morphology at the end of each run was strongly conditioned by the initial bed, which dictated flow resistance and the spatial variability of sediment mobility. During the first run with feed (R2), lateral bars developed and dictated the evolution of bed topography during the next runs. First, the bed aggraded over the existing bars, but as sediment storage increased and the bed filled, riffle-pool sequences were insinuated upstream.
- The initial conditions of the bed (bed topography and composition) influenced channel adjustments during each run. For example, the two runs with constant feed exhibited similar temporal patterns of sediment transport rates and bed surface textural parameters, but important differences in bed slope, overall storage capacity and final bed morphology.

In the future, it would be interesting to do frequency analysis of total and fractional transport rates, as well as of bed elevations to obtain statistics. It would also be interesting to analyze the evolution of bed morphology during each run (not only at the end) and estimate textural and roughness parameters over areas of the bed related to the bedforms identified. The data collected

during the experiment can also be used to test the performance of available transport models for sediment mixtures, such as those of Parker (1990) or Wilcock & Crowe (2003).

Future experimental work could be conducted to explore the following ideas:

- Could the results obtained in this study be reproduced or how different will they be if the same experiment is repeated?
- Analyze the effects of supply under different hydrographs. This would be very important because natural streams are usually subjected to changes in both feed and flow regime.
- Examine channel adjustments under different feed GSDs. This would be interesting given the importance of the GSD of supply relative to the bed.
- Explore the adjustments under different sequences of runs. This would be interesting given the significance of the initial bed for the results.

# References


Andrews, E.D., 1983. Entrainment of gravel from naturally sorted riverbed material. *Geological Society of America Bulletin*, 95(10), pp.1225–1231.

Andrews, E.D. & Erman, D.C., 1986. Persistence in the Size Distribution of Surficial Bed Material During an Extreme Snowmelt Flood. *Water Resources Research*, 22(2), pp.191–197.

Ashworth, P.J. & Ferguson, R.I., 1989. Size-selective entrainment of bed load in gravel bed streams. *Water Resources Research*, 25(4), pp.627–634.

Benda, L., 1990. The influence of debris flows on channels and valley floors in the Oregon Coast Range, USA. *Earth Surface Processes and Landforms*, 15(5), pp.457–466.

Beschta, R.L., 1983. Long-term changes in channel widths of the Kowai River, Torlesse Range, New Zealand. *Journal of Hydrology (New Zealand)*, 22, pp.112–122.

Brayshaw, A.C., 1984. The Characteristics and Origin of Cluster Bedforms in Coarse-Grained Alluvial Channels. In E. H. Koster & R. H. Stell, eds. *Sedimentology of Gravels and Conglomerates*. pp. 77–85.

Buffington, J.M. & Montgomery, D.R., 1999. Effects of sediment supply on surface textures of gravel-bed rivers. *Water Resources Research*, 35(11), pp.3523–3530.

Bunte, K., 2004. Gravel mitigation and augmentation below hydroelectric dams: a geomorphological perspective, Stream Systems Technology Center. USDA Forest Service, Rocky Mountain Research Station, Fort Collins, CO. , p.144.

Church, M., 1978. Palaeohydraulic reconstructions from a Holocene valley fill. In A. D. Miall, ed. *Fluvial Sedimentology.* pp. 743–772.

Church, M., Hassan, M. A. & Wolcott, J.F., 1998. Stabilizing self-organized structures in gravel-bed stream channels: Field and experimental observations. *Water Resources Research*, 34(11), pp.3169–3179.

Church, M. & Hassan, M.A., 2002. Mobility of bed material in Harris Creek. *Water Resources Research*, 38(11), pp.1–12.

Curran, J.C. & Wilcock, P.R., 2005. Effect of Sand Supply on Transport Rates in a Gravel-Bed Channel. *Journal of Hydraulic Engineering*, 131(11), pp.961–967.

Dietrich, W.E., Kirchner, J.W., Ikeda, H., & Iseya, F., 1989. Sediment supply and the development of the coarse surface layer in gravel-bedded rivers. *Nature*, 340(6230), pp.215–217.

Eaton, B.C., 2004. A graded stream response relation for bed load–dominated streams. *Journal of Geophysical Research*, 109(F3).

Eaton, B.C. & Church, M., 2009. Channel stability in bed load–dominated streams with nonerodible banks: Inferences from experiments in a sinuous flume. *Journal of Geophysical Research*, 114(F1).

Einstein, H.A., 1950. The bedload function for sediment transportation in open channel flow. *U.S. Departemnt of Agriculture technical Bulletin*, (1026), p.71.

Fenton, J.D. & Abott, J.E., 1977. Initial movement of grains on a stream bed: The effect of relative protrusion. *Proceedings of the Royal Society of London*, A(352), pp.523–537.

Von Flotow, C., 2013. *Temporal Adjustments of a Streambed Following an Episodic Sediment Supply Regime*. University of British Columbia.

Gessler, J., 1971. Beginning and ceasing of sediment motion. In H. W. Shen, ed. *River Mechanics*.

Gilbert, G.K., 1917. Hydraulic-mining debris in the Sierra Nevada, U.S. *Geol. Survey Prof. Paper*, 105.

Goff, J.R. & Ashmore, P.E., 1994. Gravel transport and morphological change in braided Sunwapta river, Alberta, Canada. *Earth Surface Processes and Landforms*, 19(3), pp.195–212.

Green, T., Beavis, S.G., Dietrich, C.R. & Jakeman, A.J., 1999. Relating stream-bank erosion to in-stream transport of suspended sediment. *Hydrological Processes*, 13(5), pp.777–787.

Harvey, B., McBain, S., Reiser, D., Rempel, L., Sklar, L. S. & Lave, R., 2005. Key uncertainties in gravel and biological research needs for effective river restoration, CALFED Science Program and Ecosystem Restoration Program Gravel Augmentation Panel report., p.99.

Hassan, M. & Zimmermann, A., 2011. Channel response and recovery to changes in sediment supply. In M. Church, P. A. Biron, & A. Roy, eds. *Gravel-bed River: Processes, Tools, Environments*. pp. 464–473.

Hassan, M.A., Smith, B.J., Hogan, D.L., Luzi, D.S., Zimmermann, A.E., & Eaton, B.C. , 2008. Sediment storage and transport in coarse bed streams: scale considerations. In H. Habersack, H. Piégay, & M. Rinaldi, eds. *Gravel-Bed River VI: From Process Understanding to River Restorations*. pp. 473–496.

Hassan, M.A., Church, M., Lisle, T.E., Brardinoni, F., Benda, L. & Grant, G.E., 2005. Sediment transport and channel morphology of small, forested streams. *Journal of the American Water Resources Association*, 41(4), pp.853–876.

Hassan, M.A. & Church, M., 2000. Experiments on surface structure and partial sediment transport on a gravel bed. *Water Resources Research*, 36(7), pp.1885–1895.

Hassan, M.A. & Woodsmith, R.D., 2004. Bed load transport in an obstruction-formed pool in a forest, gravelbed stream. *Geomorphology*, 58(1-4), pp.203–221.

Hayward, J.A., 1980. Hydrology and stream sediments in a mountain catchment. *Special Publication 17, Tussock Grasslands and Mountain Lands Institutes, Lincoln College, Canterbury, New Zealand*, p.236.

Jackson, W.L. & Beschta, R.L., 1982. A model of two-phase bedload transport in an Oregon coast range stream. *Earth Surface Processes and Landforms*, 7, pp.517–527.

Lamb, M.P., Dietrich, W.E. & Venditti, J.G., 2008. Is the critical Shields stress for incipient sediment motion dependent on channel-bed slope? *Journal of Geophysical Research: Earth Surface*, 113(F2).

Lane, S.N., Richards, K.S. & Chandler, J.H., 1995. Morphological estimation of the time integrated bedload transport rate. *Water Resources Research*, 31(3), pp.761–772.

Lisle, T., 1989. Sediment transport and resulting deposition in spawnning gravels, North Coastal California. *Water Resources Research*, 25(6), pp.1303–1319.

Lisle, T.E., Cui, Y., Parker, G., Pizzuto, J. E., & Dodd, A. M., 2001.The dominance of dispersion in the evolution of bed material waves in gravel-bed rivers. *Earth Surface Processes and Landforms*, 26(13), pp.1409–1420.

Lisle, T.E. & Church, M., 2002. Sediment transport-storage relations for degrading, gravel bed channels. *Water Resources Research*, 38(11).

Lisle, T.E., Iseya, F. & Ikeda, H., 1993. Response of a channel with alternate bars to a decrease in supply of mixed-size bedload: a flume experiment. *Water Resources Research*, 29(11), pp.3623– 3629.

Lisle, T.E. & Madej, M.A., 1992. Spatial variation in armouring in a channel with high sediment supply. In P. Billi et al., eds. *Dynamics of Gravel-bed Rivers.* Wiley and Sons, pp. 277–311.

Little, W.C. & Mayer, P.C., 1976. Stability of channel beds by armoring. *Journal of the Hydraulics Division -ASCE*, 102(11), pp.1647–1661.

Madej, M.A. , Sutherland, D. G., Lisle, T. E., & Pryor, B., 2009. Channel responses to varying sediment input: A flume experiment modeled after Redwood Creek, California. *Geomorphology*, 103(4), pp.507–519.

Madej, M.A. & Ozaki, V., 1996. Channel response to sediment wave 1030 propagation and movement, Redwood Creek, California, USA. *Earth Surface Processes and Landforms*, 21(10), pp.911–927.

Marr, J.D.G. Gray, J. R., Davis, B. E., Ellis, C., & Johnson, S., 2010. Large-Scale Laboratory Testing of Bedload-Monitoring Technologies : Overview of the StreamLab06 Experiments. In J.R. Gray, J. B. Laronne, & J.D.G. Marr, eds. *Bedload-surrogate monitoring technologies: U.S. Geological Survey Scientific Investigations Report 2010-5091*. pp. 266–282.

Meade, R.H., 1982. Sources, sinks and storage of river sediment in the Atlantic drainage of the United States. *Journal of Geology*, 90(3), pp.235–52.

Milhous, R.T., 1973. *Sediment transport in a gravel-bottomed stream*. Oregon State University.

Nelson, P., Venditti, J. G., Dietrich, W. E., Kirchner, J. W., Ikeda, H., Iseya, F., & Sklar, L. S., 2009. Response of bed surface patchiness to reductions in sediment supply. *Journal of Geophysical Research*, 114.

Oldmeadow, D.F. & Church, M., 2006. A field experiment on streambed stabilization by gravel structures. *Geomorphology*, 78, pp.335–350.

Papanicolaou, A.N., Tsakiris, A.G. & Strom, K.B., 2012. The use of fractals to quantify the morphology of cluster microforms. *Geomorphology*, 139-140, pp.91–108.

Parker, G., 1990. Surface-based bedload transport relation for gravel rivers. *Journal of Hydraulic Research*, 28(4), pp.417–436.

Parker, G., 2007. Transport of gravel and sediment mixtures. Sedimentation Engineering, ASCE Manuals and Reports on Engineering Practice No. 54.

Parker, G., Hassan, M.A. & Wilcock, P.R., 2008. Adjustment of the bed surface size distribution of gravel-bed rivers in response to cycled hydrographs. In H. Habersack, H. Piégay, & M. Rinaldi, eds. *Gravel-Bed Rivers VI: From Process Understanding to River Restoration*. pp. 241–289.

Parker, G. & Klingeman, P., 1982. On Why Gravel Bed Streams Are Paved. *Water Resources Research*, 18(5), pp.1409–1423.

Parker, G., Sundararajan, D. & Heinz, S., 1982. Model Experiments on Mobile , Paved Gravel Bed Streams. *Water Resources Research*, 18(5), pp.1395–1408.

Parker, G. & Wilcock, P., 1993. Sediment feed and recirculating flumes: fundamental difference. Journal of Hydraulic Engineering-ASCE, 119(11), pp.1193–1204.

Reid, L.M. & Dunne, T., 2003. Sediment budgets as an organizing framework in fluvial geomorphology. In G. M. Kondolf & H. Piegay, eds. *Tools in Fluvial Morphology*. pp. 463–500.

Roberts, R.G. & Church, M., 1986. The sediment budget in severely 1050 disturbed watersheds, Queen Charlotte Ranges, British Columbia. *Canadian Journal of Forest Research*, 16(5), pp.1092–1106.

Roering, J.J., Kirchner, J.W. & Dietrich, W.E., 1999. Evidence for nonlinear, diffusive sediment transport on hillslopes and implications for landscape morphology. *Water Resources Research*, 35(3), pp.853–870.

Ryan, S.E., 2001. The Influence of sediment supply on rates of bed load transport: a case study of three streams on the San Juan National Forest. In *Proceeding of the Seventh Federal Interagency Sedimentation Conference, March 25–29, 2001, Reno, Nevada, III-48–III-54.*

Shields, A., 1936. *Application of similarity principles and turbulence research to bed-load movement*.

Sklar, L.S., Fadde, J., Venditti, J. G., Nelson, P., Wydzga, M. A., Cui, Y., & Dietrich, W. E., 2009. Translation and dispersion of sediment pulses in flume experiments simulating gravel augmentation below dams. *Water Resources Research*, 45(8).

Smith Pryor, B., Lisle, T., Sutherland Montoya, D., & Hilton, S., 2011. Transport and storage of bed material in a gravel-bed channel during episodes of aggradation and degradation: a field and flume study. *Earth Surface Processes and Landforms*, 36(15), pp.2028–2041.

Strom, K.B. & Papanicolaou, A.N., 2007. ADV Measurements around a Cluster Microform in a Shallow Mountain Stream. *Journal of Hydraulic Engineering,*, 133(12), pp.1379–1389.

Strom, K.B. & Papanicolaou, A.N., 2008. Morphological characterization of cluster microforms. *Sedimentology*, 55, pp.137–153.

Sutherland, D.G., Ball, M.H., Hilton, S.J., & Lisle, T.E., 2002. Evolution of a landslide-induced sediment wave in the Navarro River, California. *Geological Society of America Bulletin*, 114, pp.1036–1048.

Swanson, F.J., Janda, R.J. & Dunne, T., 1982. Summary: Sediment budgets and routing in forested drainage basins. In F. J. Swanson et al., eds. *Sediment Budgets and Routing in Forested Drainage Basins*.

Trimble, S.W., 1981. Changes in sediment storage in the Coon Creek basin, Driftless area, Wisconsin, 1853 to 1975. *Science*, 214(4517), pp.181–183.

Venditti, J.G., Dietrich, W.E., Nelson, P. A., Wydzga, M. A., Fadde, J., & Sklar, L., 2010a. Effect of sediment pulse grain size on sediment transport rates and bed mobility in gravel bed rivers. *Journal of Geophysical Research*, 115(F3).

Venditti, J.G., Dietrich, W.E., Nelson, P. A., Wydzga, M. A., Fadde, J., & Sklar, L., 2010b. Mobilization of coarse surface layers in gravel-bedded rivers by finer gravel bed load. *Water Resources Research*, 46(7).

Venditti, J.G., Nelson, P.A. & Dietrich, W.E., 2008. The domain of bedload sheets. In D. Parsons, J. L. Best, & A. Trentesaux, eds. *Marine and River Dune Dynamics*. pp. 315–321.

Whipple, K.X. & Tucker, G.E., 2002. Implications of sediment-flux-dependent river incision models for landscape evolution. *Journal of Geophysical Research*, 107(B2).

Whiting, P.J., Dietrich, W. E., Leopold, L. B., Drake, T. G., & Shreve, R. L., 1988. Bedload sheets in heterogeneous sediment. *Geology*, 16(22), pp.105–108.

Wilcock, P., 1992. Experimental investigation of the effect of mixture properties on transport dynamics. In P. Billy et al., eds. *Dynamics of Gravel-Bed Rivers*. pp. 109–131.

Wilcock, P. & McArdell, B.W., 1993. Surface-based fractional transport rates: Mobilization thresholds and partial transport of a sand-gravel sediment. *Water Resources Research*, 29(4), pp.1297–1312.

Wilcock, P.R. & Crowe, J.C., 2003. A surface-based transport model for sand and gravel. *Journal of Hydraulic Engineering*, 192(2), pp.120–128.

Wilcock, P.R. & Detemple, B.T., 2005. Persistence of armor layers in gravel-bed streams. *Geophysical Research Letters*, 32(8), pp.1–4.

Wilcock, P.R., Kenworthy, S.T. & Crowe, J.C., 2001. Experimental study of the transport of mixed sand and gravel. *Water Resources Research*, 37(12), pp.3349–3358.

Wolman, M.G., 1967. A cycle of sedimentation and erosion in urban river channels 49, 385–395. *Geogr. Ann.*, 49, pp.385–395.

Zimmermann, A.E., Church, M. & Hassan, M.A., 2008. Video-based gravel transport measurements with a flume mounted light table. *Earth Surface Processes and Landforms*, 33, pp.2285–2296.